ELSEVIER

Prog. Polym. Sci. 27 (2002) 191–254

PROGRESS IN
POLYMER SCIENCE

www.elsevier.com/locate/ppolysci

Rate coefficients of free-radical polymerization deduced from pulsed laser experiments

Sabine Beuermann, Michael Buback*

Institute of Physical Chemistry, Georg-August-University Göttingen, Tammannstrasse 6, D-37077 Göttingen, Germany

Received 25 March 2001; revised 30 June 2001; accepted 9 July 2001

Abstract

Pulsed laser techniques have enormously improved the quality by which rate coefficients of individual steps in free-radical polymerization may be measured. Pulsed laser initiated polymerization (PLP) in conjunction with size-exclusion chromatography (SEC) yields the propagation rate coefficient, k_p. The PLP-SEC-technique has been applied to a wide variety of homopolymerizations and copolymerizations, either in bulk or in solution. In addition to reporting kinetic data, experimental details of PLP, of SEC, and of the limitations associated with the accurate determination of the MWD are discussed. The single pulse (SP)-PLP method, which combines PLP with time-resolved NIR spectroscopy, allows for a very detailed insight into the termination rate coefficient, k_t, for homo- and copolymerizations. k_t data are reported as a function of temperature, pressure, monomer conversion, solvent concentration, and partly also of chain length. This review considers literature up to December 2000.

Keywords: Pulsed laser induced polymerization; Homopolymerization; Copolymerization; Propagation rate coefficients; Termination rate coefficients

Contents

* Corresponding author.
E-mail addresses: mbuback@gwdg.de (M. Buback), sbeuerm@gwdg.de (S. Beuermann).

0079-6700/02/$ - see front matter
PII: S0079-6700(01)00049-1

1. Introduction

In contrast to the enormous technical importance of free-radical polymerization, the detailed understanding of polymerization kinetics is rather incomplete. For most polymerization reactions, individual rate coefficients, especially those concerning the propagation, k_p, and termination, k_t, steps which, together with initiation kinetics and initial concentrations, determine the monomer conversion vs. time dependence, are not precisely known. This can be easily seen by inspection of the *Polymer Handbook* [1] where, even for ostensibly the same polymerization conditions, widely scattering rate coefficients are tabulated. Rate coefficients also need to be known in order to describe and to simulate the polymer molecular weight (distribution), which in turn affects the properties of the polymeric material.

With the advent of pulsed-laser-assisted techniques, the unfavorable situation associated with the limited knowledge of accurate rate coefficients k_p and k_t for free-radical polymerizations has enormously improved. For most common monomers and also for several unusual ones, rate coefficients have become available. The basic principle behind the eminent success of pulsed lasers being applied toward measuring

Nomenclature

AA	acrylic acid
AIBN	azobisisobutyronitrile
AN	acetonitrile
BA	butyl acrylate
BMA	butyl methacrylate
BzOH	benzyl alcohol
CO_2	carbon dioxide
CHMA	cyclohexyl methacrylate
DA	dodecyl acrylate
DDM	*n*-dodecyl mercaptan
DMA	dodecyl methacrylate
DMF	dimethyl formamide
DMPA	2,2-dimethoxy-2-phenylacetophenone
DMSO	dimethyl sulfoxide
EHMA	2-ethylhexyl methacrylate
EMA	ethyl methacrylate
EMK	ethyl methyl ketone
EtOH	ethanol
GMA	glycidyl methacrylate
HAc	acetic acid
HEMA	hydroxyethyl methacrylate
HPMA	2-hydroxypropyl methacrylate
*i*BMA	*i*-butyl methacrylate
*i*BoMA	*i*-bornyl methacrylate
*i*DeMA	*i*-decyl methacrylate
MA	methyl acrylate
MAA	methacrylic acid
MAN	methacrylonitrile
MeOH	methanol
MES	mesitylene
MIB	methyl isobutyrate
MMA	methyl methacrylate
NIPAM	*N*-isopropylacrylamide
NMP	*N*-methyl pyrrolidinone
OAc	*n*-octyl acetate
PAA	poly(acrylic acid)
PCS	*p*-chlorostyrene
PMA	poly(methyl acrylate)
PMAA	poly(methacrylic acid)
PMMA	poly(methyl methacrylate)
PMOS	*p*-methoxystyrene

PS	polystyrene
PVAc	poly(vinyl acetate)
S	styrene
TOL	toluene
TRIS	3-[tris(trimethylsilyloxy)silyl] propyl methacrylate
VAc	vinyl acetate
VEOVA	vinyl *neo*-decanoate

free-radical polymerization rate coefficients consists of the ease and the effectiveness by which UV laser pulses of several nanoseconds duration may instantaneously create pre-selected free-radical concentrations or generate free-radical concentration profiles. In principle, irradiation with a flash lamp [2] or, especially for applications on heterogeneous systems, with an electron beam source [3,4] may also be used to externally control free-radical polymerization. These techniques are, however, less easily applied and the time-resolution of pulse-initiation by a flash lamp cannot compete with what can be reached by using a UV laser. For this reason, the paper will only deal with pulsed laser techniques using UV initiation mostly from an excimer laser source.

Two such methods are of particular importance: the PLP–SEC method uses pulsed-laser polymerization (PLP) in conjunction with size-exclusion chromatographic (SEC) analysis of the polymeric material. The pulsed laser light almost instantaneously creates an intense burst of free radicals. Varying the laser pulse repetition rate allows for producing generations of primary free radicals at pre-selected time intervals. The pulsing translates into a characteristic pattern of the molecular weight distribution (MWD). Analysis of the MWD enables the unambiguous determination of the propagation rate coefficient, k_p. Aspects of PLP along these lines were first put forward by Aleksandrov et al. [5]. It is, however, the pioneering work of Olaj and coworkers [6,7] by which the application of pulsed laser techniques toward k_p measurement was demonstrated. In Section 2, the PLP–SEC method will be outlined and the investigations into k_p of homo- and copolymerizations will be reviewed.

Within the second method, polymerization induced by a single laser pulse (SP) is monitored via on-line infrared or near-infrared spectroscopy with a time resolution of microseconds [8]. From the measured trace of monomer conversion vs. time (after applying the laser pulse), the ratio of termination to propagation rate coefficients, k_t/k_p, is obtained which, together with k_p from PLP–SEC, yields individual k_t values over extended ranges of monomer conversion. The aspects of this so-called SP–PLP technique will be detailed in Section 3.

During recent years, single-pulse techniques in conjunction with the analysis of the resulting polymer MWD have been developed and tested by Olaj et al. [9] and by deKock [10]. A review on such studies which are directed toward measuring chain-length dependendent k_t is given in Ref. [11]. These investigations are restricted to small initial conversions and thus will not be addressed in detail. Aspects of measuring the chain-length dependence of k_t via SP–PLP will be briefly outlined in Section 3.7.

Although PLP–SEC experiments are primarily devoted to k_p measurement, they also yield information about k_t [6,7,12–15] and about transfer rate coefficients [16]. These aspects will be briefly mentioned in the final part of Section 2. Similarly, as will be shown in Section 3, the SP–PLP data, in addition to providing k_t values, contains information about k_p. To extract the full informational

content, it is recommendable to accompany PLP experiments by simulations [17]. The PREDICI® program package [18] has been successfully applied for this purpose.

The majority of PLP experiments carried out so far are PLP–SEC studies into homopolymerizations with several groups around the world being engaged in these efforts. SP–PLP studies, on the other hand, have only been performed at Göttingen University. One reason for SP–PLP studies not being so widespread is that this experiment is more difficult in that the (mostly rather small) monomer conversion induced by a SP needs to be precisely detected under polymerization conditions with microsecond time resolution. The PLP–SEC experiment is less demanding in that only the laser pulsing has to be carried out under actual polymerization conditions whereas the analysis of polymer molecular weight may be performed by SEC under standard conditions at any time after PLP. From both methods, PLP–SEC and SP–PLP, a large amount of rate coefficient data has accumulated during recent years. It is the purpose of this article to present an overview of these results.

2. PLP–SEC experiments directed toward the determination of propagation rate coefficients

After a brief consideration of the PLP–SEC experiment, propagation rate coefficient data determined from this technique for free-radical homo- and copolymerizations will be given. The majority of this data refers to bulk polymerizations, but k_p in solution will also be addressed.

2.1. Experimental considerations

Within Section 2.1 experimental aspects of the PLP–SEC procedure will be outlined.

2.1.1. Pulsed-laser initiated polymerizations

In PLP experiments, an evenly spaced sequence of laser pulses, mostly at a UV wavelength, is applied to a reaction system which contains monomer and a photoinitiator. Acetophenones or benzoin is most frequently used as initiators. Azoinitiators should only be used in case of very slowly propagating monomers as photodecomposition of the initiator may not be instantaneous [19]. The number of pulses is chosen such as to yield a small initial monomer conversion, typically of 2–3%. The almost instantaneous production of a large amount of primary initiator-derived free radicals by each laser pulse causes an enhanced termination probability for radicals from the preceding pulse(s) resulting in a periodically changing radical concentration vs. time profile. This periodic variation in free-radical concentration, c_R, may lead to a structured MWD. At present, these MWDs are best determined from SEC. As an example, Fig. 1 gives an MWD for poly(dodecyl acrylate) obtained from a PLP experiment at −4 °C and 200 bar in the presence of 36 wt% CO_2. The laser pulse repetition rate was 100 Hz. The MWD exhibits two distinct maxima at $\log M = 4.8$ and $\log M = 5.1$ and an additional shoulder around $\log M = 5.2$.

The propagation rate coefficient k_p is derived from the MWD according to Eq. (1)

$$L_i = ik_p c_M t_0 \qquad i = 1, 2, 3, \ldots \tag{1}$$

where L_1 and t_0 are the number of propagation steps and the time interval between two successive laser pulses, respectively, and c_M is the monomer concentration. Higher-order inflection points, L_2, L_3, L_4,…, result from preferential termination of the propagating radicals generated at $t = 0$ by laser pulses applied at times $2t_0$, $3t_0$, $4t_0$,…, respectively. A consensus has emerged that in general L_1 may be best identified with

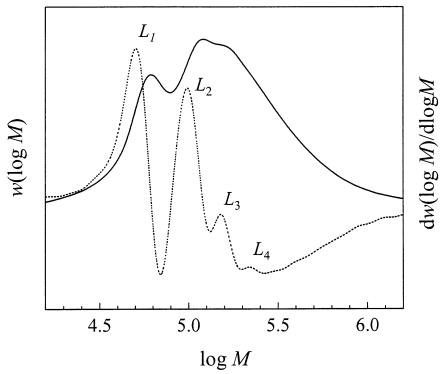

Fig. 1. MWD for poly(dodecyl acrylate) obtained at −4 °C, 200 bar, and a laser pulse repetition rate of 100 Hz in 36 wt% CO_2 (full line) and corresponding first derivative plot of the MWD (dotted line).

the first inflection point on the low molecular weight side of the MWD peak [20,21]. In practice, the inflection point is determined as the maximum of the first derivative of the MWD curve, which is given as the dashed line in Fig. 1. Four distinct maxima are clearly observed. They are assigned to L_1, L_2, L_3, and L_4.

As has been pointed out in papers published by the IUPAC Working Party *Modeling of polymerization kinetics and processes* the PLP–SEC technique provides self-consistency checks for the determination of reliable k_p data [20–22]. For example, it has to be checked whether identical k_p values are obtained upon variation of experimental parameters such as laser pulse repetition rate, photoinitiator concentration, and laser pulse energy. The most important consistency check, however, is the occurrence of at least a secondary inflection point (L_2 in Fig. 1) located at twice the molecular weight of the first inflection point. The occurrence of higher-order inflection points clearly indicates that the MWD is determined by the periodically changing radical concentration. Eq. (1) demonstrates the linear dependence of the characteristic chain-length L_1 on t_0, the time between two successive laser pulses. If chain-stopping and chain-starting events are not essentially controlled by laser pulsing, this correlation is lost. Thus in cases where chain-transfer is significant or where the termination rate is very high, k_p is not easily accessible from PLP–SEC.

For monomers such as styrene and methacrylic acid esters, well structured MWDs, as presented in Fig. 1, are obtained for a wide range of temperature, pressure, initiator concentrations, monomer concentrations, and laser pulse repetition rates [20–22]. However, for several other monomers it has been proven difficult to identify reaction conditions under which MWDs suitable for k_p determination may be obtained. Based on simulations of PLP experiments, the origin of these difficulties will be illustrated below and suggestions will be made under which reaction conditions k_p might be available from PLP studies.

The shape of the MWD is determined by several rate coefficients, the primary radical concentration (c_R^0) and time t_0, which is given by $t_0 = \nu_R^{-1}$, where ν_R is the laser pulse repetition rate. The time dependence of c_R and the MWDs for different types of PLPs, as obtained from PREDICI® simulation, are given in Figs. 2–4. The modeling is based on the following simplified reaction scheme

- Initiation

$$I \xrightarrow{h\nu} 2R_I$$

$$R_I + M \xrightarrow{k_I} R_1$$

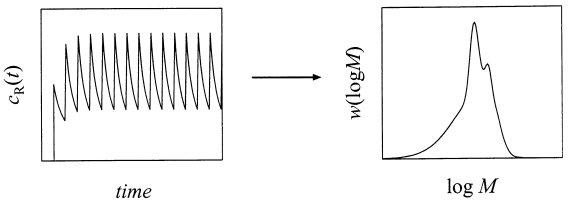

Fig. 2. Radical concentration–time profile (left) and resulting molecular weight distribution obtained from simulations with the rate coefficients given for Case 1 in the text.

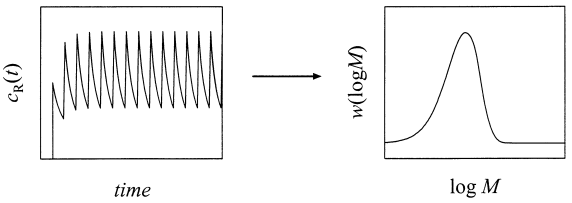

Fig. 3. Radical concentration–time profile (left) and resulting molecular weight distribution obtained from simulations with the rate coefficients given for Case 2 in the text.

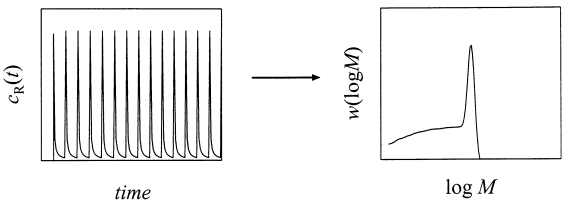

Fig. 4. Radical concentration–time profile (left) and resulting molecular weight distribution obtained from simulations with the rate coefficients as given for Case 3 in the text.

- Propagation

$$R_n + M \xrightarrow{k_p} R_{n+1}$$

- Termination

$$R_n + R_m \xrightarrow{k_t} P_n + P_m$$

- Chain transfer to monomer

$$R_n + M \xrightarrow{k_{tr,M}} P_n + R_1$$

where I is the initiator, R_I an initiator-derived radical, R_1 is a small radical with one monomeric unit at the chain end, R_n, a radical of chain length n, M, the monomer, and P_n, the polymer of chain length n. k_p, k_t, and $k_{tr,M}$ are the rate coefficients for propagation, termination and chain transfer to monomer,

respectively. The simulations have been carried out for a concentration of the primary radical R_I of $c_R^0 = 1 \times 10^{-6}$ mol l^{-1} being generated by each laser pulse with the pulses being applied at a repetition rate of 10 Hz. The simulations are based on the assumption that the formation of initiator-derived radicals R_I proceeds instantaneously as compared to the subsequent processes of the R_I radicals. The kinetic coefficients are: $k_I = k_p = 600$ l mol^{-1} s^{-1} and $k_t = 1 \times 10^7$ l mol^{-1} s^{-1}. The termination reaction is considered to proceed only via disproportionation. It has been shown by simulation that the type of termination reaction (recombination vs. disproportionation) and the size of the associated termination rate coefficients do not disturb the PLP structure of the MWD [23]. Figs. 2–4 give the c_R–t profiles and the MWDs modeled for the following three cases:

Case 1 comprises the situation of monomers with propagation rate coefficients in the range of some hundreds up to 10^3 l mol^{-1} s^{-1} and with low chain transfer to monomer rate coefficients, $k_{tr,M}$, which, e.g. occurs with styrene and methacrylates. The modeling results for Case 1 with $k_{tr,M} = 0$ are presented in Fig. 2.

Case 2 considers systems where the rate coefficient of the chain-transfer to monomer reaction is high. The modeling (Fig. 3) has been carried out with $k_{tr,M} = 2$ l mol^{-1} s^{-1}.

Case 3 describes the influence of the termination rate on the MWD. The simulations (Fig. 4) were performed with the same set of coefficients as in Case 1, but with the termination rate coefficient being increased by a factor of 20 to $k_t = 2 \times 10^8$ l mol^{-1} s^{-1}.

The c_R vs. time t-profiles in Figs. 2 and 3 are the same since the chain-transfer reaction does not influence free-radical concentration. However, the MWDs given on the right-hand-side (RHS) of the figures exhibit clear differences. Whereas the MWD for Case 1 (Fig. 2) shows a distribution with two distinct peaks, a uniform MWD is seen in Case 2 (Fig. 3). Due to the significance of the chain-transfer to monomer reaction, the linear correlation between t_0 and the chain length of the propagating radical is lost. As a result, reliable k_p values cannot be determined if Case 2 applies.

The modeling results for high termination rate (Case 3) show clear differences as compared to Cases 1 and 2. The majority of radicals formed by one pulse are terminated before the subsequent pulse arrives. As a consequence, the correlation of macroradical chain-length with t_0 is lost. Due to the high termination rate, a very sharp, structureless MWD is obtained. k_p values are not unambiguously accessible under these conditions.

These examples demonstrate that reaction conditions for reliable k_p determination from PLP–SEC experiments have to be optimized. Strategies of finding adequate PLP conditions will be given in Sections 2.2.3 and 2.2.4, which refer to the more complicated acrylate and vinyl ester systems, respectively.

2.1.2. Size-exclusion chromatographic analysis of polymer from PLP

The determination of propagation rate coefficients from PLP–SEC requires the knowledge of absolute MWDs. The accuracy of k_p values is directly related to the quality of molecular weight analysis. In order to derive absolute molecular weights, the following strategies were applied.

(1) Absolute detection. Optimum SEC calibration is established via well-characterized narrow polydispersity standards of the polymer under investigation. This procedure is applied in the analysis of polystyrene and poly(methyl methacrylate) (PMMA) samples [20,22]. However, for many systems, especially for copolymers, well-characterized polymer standards are not available.

(2) Procedure via universal calibration. In cases where molecular weight standards for the particular

polymer are not available, the PLP samples may be analyzed by using the principle of universal calibration [24]: After calibrating the SEC set-up with either PS or PMMA standards, the MWD of the polymer sample is calculated using a transformation procedure that requires two sets of Mark–Houwink parameters: one for the polymer used for calibration and one for the polymer under investigation [25]. Thus, the accuracy of the derived k_p values strongly depends on the accuracy of the two sets of Mark–Houwink parameters and special care has to be taken in determining these parameters. A detailed discussion is given by Jackson et al. [26].

(3) Multi-detector SEC. Another direct determination of the MWD uses an SEC system with multiple detectors, most commonly refractive index measurement in combination with on-line viscometry or on-line light scattering. Such a set-up directly yields absolute polymer molecular weights. A more detailed comparison of the two SEC calibration procedures is beyond the scope of this study. For a discussion of the problems that may occur with this strategy, the reader is referred to the publications by the group of Davis [27]. As compared to the direct SEC calibration methods as employed for styrene and MMA PLP studies, additional calibration procedures are required for molecular weight analysis via methods 2 and 3. It is important to be aware that such extra steps enhance the uncertainty of k_p measurements via PLP–SEC.

(4) Polymer fractionation by SEC and MALDI analysis. In addition to the above described calibration strategies, SEC may also be used to fractionate polymer samples, which are subsequently analyzed by MALDI, thus providing absolute molecular weights. Due to the fractionation of the polymer, samples with very narrow distributions are obtained and problems of MALDI analysis for broad polymers are omitted [28]. This method has, however, not been extensively used so far.

The four methods of measuring absolute MWDs are applicable to homo- and copolymers. It should, however, be noted that k_p studies for copolymerizations require SEC calibration for each copolymer composition under investigation. The MALDI technique has already been used to characterize biopolymers [29].

There are other factors beyond SEC calibration, which influence the accuracy of measured k_p data. The type of MWD from which the inflection points are derived may also play a role. In most PLP–SEC studies, the logarithmic MWD, $w(\log M)$, directly obtained from SEC analysis employing a mass detector, is used to derive k_p. As has been shown in Refs. [6,7], the position of inflection points may be directly read from the $w(\log M)$ distribution. For most of the systems studied so far, the $w(\log M)$ distribution provides more distinct inflection points than do the other distributions, such as the $w(M)$-distribution or the number distribution, $f(M)$. An extensive theoretical study, on factors influencing the quality of k_p determination [17] revealed that the logarithmic MWD provides the most robust access to the inflection points. This finding is based on modeling of PLP–SEC experiments for a range of pulsed laser induced free-radical concentrations. In Ref. [17], it was shown that the position of the inflection points on the $w(\log M)$-distribution is less prone to experimental SEC broadening and thus k_p data are less affected.

It should be noted that at high concentrations of laser induced free-radicals, c_R^0, and thus at high termination rate, under conditions of the so-called 'high termination rate limit' [30,31], the peak maximum of the MWD may be a better measure for L, the number of propagation steps between two successive laser pulses. However, these high values of c_R^0 are difficult to achieve experimentally. In addition, it is not easy to judge whether the high termination limit is truly operative. In acrylate polymerizations, even by scanning c_R^0 over a wide range, the 'high termination rate limit' could not be reached [32].

For a detailed discussion of experimental details the reader is referred to Refs. [20–22].

Table 1
Monomers subjected to PLP–SEC investigations

Monomer	Variation		Bulk/solvent	Reference
	T	*p*		
Styrene	x	x	Bulk, BzOH, NMP, AN, DMF, MIB, toluene, anisole, benzene, DMSO, bromobenzene, cyclohexane, MES, 1,2-dichloroethane, acetonitrile, CO_2	[22,27,33–40]
4-Methylstyrene	x		Bulk	[35]
4-Fluorostyrene	x		Bulk	[35]
4-Chlorostyrene	x		Bulk	[35]
4-Bromostyrene	x		Bulk	[35]
4-Methoxystyrene	x		Bulk	[35]
MMA	x	x	Bulk, BzOH, NMP, AN, DMF, toluene, anisole, MIB, bromobenzene, benzene, MES, 1,2-dichloroethane, cyclohexane, DMSO, EMK, MeOH, EtOH, CO_2	[20,27,34,36,38,39,41–45]
EMA	x		Bulk	[21,27,46,47,67]
BMA	x	x	Bulk, 2-heptanone	[21,25,27,46,48,67]
*i*BMA	x		Bulk	[67]
EHMA	x		Bulk	[67]
iDMA	x		Bulk	[67]
DMA	x	x	Bulk, 2-heptanone, OAc	[21,25,47,48,67]
BzMA	x		Bulk	[27,68]
CHMA	x	x	Bulk, 2-heptanone, OAc	[68,69]
*i*BoMA	x		Bulk	[68]
HEMA	x	x	Bulk	[69]
HPMA	x		Bulk	[68]
GMA	x	x	Bulk	[68,69]
TRIS	x		Bulk	[49]
MAN	x		Bulk	[50]
MAA	x		Bulk, MeOH, toluene, THF, HAc	[51,52]
MA	x		Bulk, CO_2	[53–55]
BA	x	x	Bulk, THF, CO_2	[32,56,57]
EHA	x		Bulk	[32]
DA	x	x	Bulk, CO_2	[54,55]
NIPAM	x		Water	[58]
AA	x		Water	[52,59]
VAc	x	x	Bulk, *t*-BuOH, CO_2	[53,60–62]
VEOVA	x		Bulk	[63]
Chloroprene	x		Bulk	[64]
1,3-Butadiene	x		Chlorobenzene	[2]
Ethyl α-hydroxy methacrylate			Benzene, butanone, chlorobenzene, chloroform, cyclohexane, ethanol, dichloromethane, ethyl acetate, THF, pentan-1-ol, propan-1-ol, toluene, xylene, ethyl benzene	[65]
Dimethyl itaconate	x		Bulk	[66]

2.2. Propagation rate coefficients in homopolymerizations

Propagation rate coefficients have been determined for a large number of monomers applying the PLP–SEC technique. To the best of our knowledge, Table 1 gives a compilation of all monomers, which were studied with the PLP–SEC technique so far, with publications until December 2000 being considered. Table 1 indicates for which monomers a variation of temperature and pressure was performed. In addition, the reaction medium, bulk or solution, is listed.

For a detailed discussion of the experimental data, the monomers are grouped into the following categories: styrene and substituted styrenes, methacrylic acid esters, acrylic acid ester, vinyl esters, olefins, and others. The results for these groups are discussed in Sections 2.2.1–2.2.6. In Section 2.2.7, a comparison of k_p for monomers belonging to different families is given. For error estimates of the rate coefficients and activation parameters the reader is referred to the cited original literature.

2.2.1. Styrene and substituted styrenes

The monomer which has most extensively been studied by the PLP–SEC technique is styrene. Critically evaluated propagation rate coefficients for bulk polymerizations, so-called 'benchmark values', have been compiled by the IUPAC Working Party *Modeling of kinetics and processes of polymerization* [22]. The following Arrhenius equation for k_p has been derived from k_p data originating from nine research groups:

$$\text{styrene}: \qquad \ln k_p\ (\mathrm{l\ mol^{-1}\ s^{-1}}) = 17.57 - 3909(T^{-1}\ (\mathrm{K^{-1}})) \qquad (-12\ ^\circ\mathrm{C} < \Theta < 93\ ^\circ\mathrm{C}) \qquad (2)$$

with a pre-exponential factor of $A = 4.27 \times 10^7$ l mol^{-1} s^{-1} and activation energy of $E_A = 32.5$ kJ mol^{-1}. Additionally, investigations into the pressure dependence of k_p have been reported [33]. According to the general expression for the activation volume $\Delta V^{\#}$ (Eq. (3)), $\Delta V^{\#}(k_p)$ for styrene at 30 °C has been found to be -12.1 cm^3 mol^{-1}

$$\frac{\mathrm{d}\ln k}{\mathrm{d}p} = \frac{\Delta V^{\#}}{RT} \qquad (3)$$

With k_p being given in the typical units of l mol^{-1} s^{-1}, the activation volume shows a slight variation with temperature, e.g. $\Delta V^{\#}(k_p, 90\ ^\circ\mathrm{C}) = -11.1$ cm^3 mol^{-1}. k_p data of styrene homopolymerization from 30 to 90 °C and from ambient pressure to 2800 bar has been fitted to the following equation:

$$\ln k_p\ (\mathrm{l\ mol^{-1}\ s^{-1}}) = 17.14 - 1.873 \times 10^{-4} p\ (\mathrm{bar}) - \frac{3748}{T\ (\mathrm{K})} + \frac{0.202}{T\ (\mathrm{K})} p\ (\mathrm{bar}) \qquad (4)$$

It should be noted that with propagation rate coefficients being expressed as k_p^*, which are in units of kg mol^{-1} s^{-1}, the temperature dependence of the activation volumes $\Delta V^{\#}(k_p^*)$ is less pronounced [33].

For several *para*-substituted styrenes, the temperature dependence of k_p has been studied by PLP–SEC [35]. Table 2 contains the ambient pressure k_p values at 40 °C and the Arrhenius parameters for these monomers. The entries refer to the notations in Eq. (5)

$$\ln k_p = \ln A - E_A/RT \qquad (5)$$

k_p values increase by more than a factor of two in going from *p*-methoxystyrene to *p*-bromostyrene, with k_p for styrene being in between these two values. The activation energies for *para*-methylstyrene, *para*-fluorostyrene, and *para*-chlorostyrene are not significantly different from the styrene value. For *para*-bromostyrene and *para*-methoxystyrene slightly higher activation energies of about 34 kJ mol^{-1} are observed. However, as stated in Ref. [35], it is not possible to discriminate whether the substituent

Table 2
Propagation rate coefficients at 40 °C, k_p (40 °C), and Arrhenius parameters, A and E_A, obtained for bulk homopolymerizations of *para*-substituted styrenes at ambient pressure [35]

	4-Methoxystyrene	4-Methylstyrene	Styrene	4-Fluorostyrene	4-Chlorostyrene	4-Bromostyrene
k_p (40 °C) (l mol^{-1} s^{-1})	94	112	160	159	197	212
E_A (kJ mol^{-1})	34.9	32.4	31.5	32.0	32.1	33.9
$A \times 10^{-7}$ (l mol^{-1} s^{-1})	6.35	2.84	2.88	3.50	4.48	9.57

Table 3
Propagation rate coefficients at 50 °C, k_p (50 °C), and Arrhenius parameters, A and E_A, obtained for bulk homopolymerizations of *n*-alkyl methacrylates at ambient pressure; Θ interval indicates the temperature range in which the data has been measured (Activation volumes $\Delta V^{\#}$ are measured at 30 °C)

Monomer	A (l mol^{-1} s^{-1})	E_A (kJ mol^{-1})	$\Delta V^{\#}$ (cm^3 mol^{-1})	k_p (50 °C) (l mol^{-1} s^{-1})	Θ Interval (°C)	Reference
MMA	2.67×10^6	22.4	−16.7[a]	648	−1 to 90	[20]
EMA	4.06×10^6	23.4	–	671	6.1 to 50	[21]
BMA	3.78×10^6	22.9	−16.5[b]	757	−20 to 90	[21]
DMA	2.50×10^6	21.0	−16.0[b]	995	9 to 90	[21]

[a] Determined at 30 °C [41].
[b] Determined at 30 °C [25].

affects the activation energy or the frequency factor. This may partly be due to the narrow temperature range (20–40 °C) employed in the experiments.

2.2.2. Methacrylic acid esters

Propagation rate coefficients for a series of *n*-alkyl methacrylates have been critically evaluated [20,21]. The k_p data for MMA, EMA, BMA, and DMA constitute benchmark value data sets. Table 3 contains the Arrhenius parameters for these monomers according to Eq. (5). The temperature range of the PLP experiments, k_p at 50 °C, and the activation volume $\Delta V^{\#}(k_p)$ are also listed.

The data in Table 3 clearly show that k_p increases with the size of the ester group. In going from the methyl to the dodecyl ester, k_p is enhanced by a factor of 1.5. As has been discussed previously, it is not possible to assign, on the basis of the presently available data, the observed trend of k_p with ester length to either the pre-exponential factor, A, to the activation energy, E_A, or to both quantities [21].

Table 4
Propagation rate coefficients at 50 °C, k_p (50 °C), and Arrhenius parameters, A and E_A, obtained for bulk homopolymerizations of methacrylates carrying branched alkyl, cyclic, or functional ester groups at ambient pressure; Θ interval indicates the temperature range in which the data has been measured. Activation volumes $\Delta V^{\#}$ are measured at 30 °C

Monomer	$A \times 10^{-6}$ (l mol^{-1} s^{-1})	E_A (kJ mol^{-1})	$\Delta V^{\#}$ (cm^3 mol^{-1})	k_p (50 °C) (l mol^{-1} s^{-1})	Θ Interval (°C)	Reference
*i*BMA	2.64	21.8	–	794	10 to 90	[67]
iDMA	2.19	20.8	–	959	10 to 90	[67]
EHMA	1.87	20.4	–	944	10 to 90	[67]
CHMA	4.88	22.3	−16.2[a]	1212	0 to 90	[69]
	3.76	21.5		1257	30 to 110	[68]
GMA	4.41	21.9	−15.0[a]	1273	−10 to 60	[69]
	6.02	22.9	–	1118	30 to 110	[68]
BzMA	3.61	21.5	–	1224	30 to 110	[68]
	8.50	23.2	–	1510	6 to 47	[27]
*i*BoMA	4.28	22.5	–	1002	30 to 110	[68]
HEMA	8.88	21.9	−15.8[a]	2563	−4 to 70	[69]
HPMA	3.51	20.8	–	1504	30 to 110	[68]
TRIS	1.44	19.9	–	871	15 to 50	[49]

[a] Determined at 30 °C.

Table 5
Propagation rate coefficients at 20 °C, k_p (20 °C), Arrhenius parameters, A and E_A, and activation volumes, $\Delta V^{\#}$ obtained for bulk homopolymerizations of *n*-alkyl acrylates at ambient pressure; Θ interval indicates the temperature range in which the data has been measured, see text for further details

Monomer	$A \times 10^6$ (l mol^{-1} s^{-1})	E_A (kJ mol^{-1})	$\Delta V^{\#}$ (cm^3 mol^{-1})	k_p (20 °C) (l mol^{-1} s^{-1})	Θ Interval (°C)	Reference
MA	–	–	−11.7[a]	–	−28 to −15	[54]
	16.6	17.7		11 600	−19 to 32	[53]
BA	15.8	17.3	–	13 100	−65 to −7	[56]
	0.74	*9.6*	–	14 200	5 to 30	[32]
	18.1	17.4	–	14 400	−65 to 30	[32,56][b]
EHA	–	–	–	16 700	5 to 25	[32]
DA	17.9[c]	17.0	−11.7[d]	16 700[c]	−3 to 30	[54]
	–	–	–	18 800	10 to 30	[32]

[a] Determined at −15 °C.
[b] Combined fit of experimental BA data from Refs. [32,56].
[c] Data determined at 100 bar and extrapolated to ambient pressure using the given $\Delta V^{\#}$.
[d] Determined at 15 °C.

In addition to the *n*-alkyl methacrylates, also methacrylates with branched alkyl, cyclic or functional ester groups were studied [67–69]. The results are contained in Table 4. For branched alkyl methacrylates such as *iso*-butyl (*i*BMA), *iso*-decyl (*i*DeMA), and 2-ethylhexyl (EHMA) methacrylate the temperature dependence was investigated. The two methacrylates with larger ester groups, *i*DeMA and EHMA, have k_p values that are very close to k_p of dodecyl methacrylate. Interestingly, k_p values determined for *i*BMA are below the values for BMA and are very close to k_p for EMA. The methacrylates with cyclic ester groups such as benzyl (BzMA), cyclohexyl (CHMA), and glycidyl methacrylate (GMA) result in almost identical k_p data, which are close to the DMA value. *iso*-Bornyl methacrylate (*i*BoMA) carrying a sterically demanding group has k_p values close to those of the higher alkyl esters, too. Monomers containing an OH-group such as 2-hydroxypropyl (HPMA) and hydroxyethyl (HEMA) methacrylate show significantly higher k_p than the other methacrylates studied so far. The agreement between results provided by different groups is generally very good, with the exception of BzMA, where the k_p values reported by Davis et al. [27] are approximately 25% below the Hutchinson et al. [68] data. In view of the scattering associated with k_p measurement via non-PLP–SEC experiments [1], even this deviation may be considered as satisfactory agreement.

For several methacrylate monomers, the pressure dependence of k_p has been studied, too. The activation volumes listed in Tables 3 and 4 are found to be in the narrow range between −15 and −17 cm^3 mol^{-1}.

Most studies into k_p of methacrylates were carried out in a temperature range where depropagation is not operative, usually at $\Theta \leq 90$ °C. PLP–SEC experiments at higher temperatures may be used to derive depropagation rate coefficients as well as enthalpies and entropies of polymerization [48].

2.2.3. Acrylic acid esters

In contrast to the methacrylate monomers, only a few alkyl esters of acrylic acid have been studied by the PLP–SEC technique. In addition, these investigations were restricted to temperatures up to 30 °C. The results for methyl (MA), butyl (BA), dodecyl (DA), and ethylhexyl (EHA) acrylate are given in Table 5. Arrhenius parameters, which have been derived from a narrow temperature range, are given in

italics. As with the methacrylates, a clear increase of k_p with ester size is observed: k_p of DA is approximately 50% higher than k_p of MA. Although being associated with quite different Arrhenius parameters, the k_p values of the two BA sets are close to each other in the overlapping temperature range. Thus, the entire data set is subjected to a combined fit. The resulting activation energy of 17.4 kJ mol^{-1} is very close to the values for MA and DA.

The pressure dependence of acrylate k_p has also been investigated. One and the same value, $\Delta V^{\#} = (-11.7 \pm 1.8)$ cm^3 mol^{-1}, is obtained as the activation volume for MA and DA (Table 5).

The following aspects have been put forward to explain why acrylate k_p is difficult to obtain for temperatures above 30 °C:

High chain-transfer to monomer and at the same time high propagation rate coefficients [32,54,70]. Chain-transfer to monomer events constitute a continuous source of small radicals, which may start chain growth at any time. In addition, transfer serves as an effective chain-stopping process, which is particularly relevant for high k_p monomers. As a consequence of both effects, chain-transfer to monomer destroys the correlation between t_0 and chain length. If the reaction conditions are changed such that the transfer-induced chain-starting and chain-stopping events are reduced, e.g. by increasing the laser pulse repetition rate [32] or by diluting the reaction system with a solvent that shows low chain-transfer activity [44,57], MWDs with PLP structure may become accessible.

Chain-transfer to polymer. At the low polymer concentrations which are typical for PLP–SEC experiments, *inter*molecular chain-transfer to polymer is not expected to play a major role, but it must not be negligible. *Intra*molecular chain-transfer may however take place from the very beginning of the polymerization reaction. The consequences of chain-transfer have not been studied in too much detail so far. The group of Lovell studied BA and vinyl acetate polymerizations at 70 °C and found significant contributions of chain transfer to polymer [71,72]. Extrapolation of that data to 30 °C indicates that such effects should be negligible at 30 °C and low degrees of monomer conversion.

Measurement of absolute MWDs by SEC analysis. In addition to the SEC-calibration issues discussed in Section 2.1.2, problems may arise from the degree of branching of the polymer under investigation. This holds especially true for cases where linear standards are used for SEC calibration or the determination of Mark–Houwink constants is based on linear polymer samples. Since separation of polymer samples is based on the differences in hydrodynamic volumes, no 'true' k_p values may be deduced even in cases where a clear PLP structure of the MWD is seen.

It should be noted that the branching tendency at high temperatures may lead to inadequate rate coefficients if low temperature PLP–SEC derived k_p values are extrapolated to high temperatures. During the branching process secondary polymeric radicals are generated, which show much lower k_p values, since they are more stable than the regular propagating acrylate radicals [73–76].

2.2.4. Vinyl esters

Vinyl acetate (VAc) and vinyl *neo*-decanoate (VEOVA) have also been investigated via PLP–SEC. As with the acrylates, both monomers require optimized reaction conditions in order to obtain MWDs, which are suitable for k_p estimates. Due to the high termination rate, with k_t being above 10^8 l mol^{-1} s^{-1}, successful PLP experiments on VAc require low initiator concentrations and/or short time delays between two successive laser pulses [60]. At these reaction conditions, k_p data for VEOVA become accessible. The Arrhenius parameters of k_p according to Eq. (5) are listed in Table 6. For VAc, also the variation of k_p with pressure was studied. At 25 °C an activation volume of (-10.7 ± 0.5) cm^3 mol^{-1} has been estimated.

Table 6
Arrhenius parameters, A and E_A, activation volume, $\Delta V^{\#}$, and propagation rate coefficients at 50 °C, k_p (50 °C) at ambient pressure, for bulk homopolymerizations of vinyl acetate (VAc) and vinyl *neo*-decanoate (VEOVA); Θ interval indicates the temperature range in which the data has been measured

Monomer	$A \times 10^6$ (l mol^{-1} s^{-1})	E_A (kJ mol^{-1})	$\Delta V^{\#}$ (cm^3 mol^{-1})	k_p (50 °C) (l mol^{-1} s^{-1})	Θ Interval (°C)	Reference
VAc	10	19.8	–	6300	10 to 56	[53]
VAc	14.7	20.7	–	6625	10 to 60	[61]
VAc	–	–	−10.7	–	–	[62]
VEOVA	20.4	22.2	–	5265	−21 to 21	[63]

2.2.5. Olefins

2.2.5.1. Chloroprene. Bulk polymerizations of chloroprene were carried out in a temperature range from 10 to 55 °C [64]. The following Arrhenius equation has been obtained:

$$\ln k_p\,(\mathrm{l\,mol^{-1}\,s^{-1}}) = 16.79 - 3199(T^{-1}\,(\mathrm{K^{-1}})), \qquad (10\,^{\circ}\mathrm{C} \le \theta \le 55\,^{\circ}\mathrm{C}) \tag{6}$$

with $A = 1.95 \times 10^7$ l mol^{-1} s^{-1} and $E_A = 26.6$ kJ mol^{-1}. At 50 °C, a k_p value of 978 l mol^{-1} s^{-1} is observed.

2.2.5.2. 1,3-Butadiene. The propagation rate coefficient for 1,3-butadiene polymerizations has been determined for reactions in chlorobenzene in a temperature range from 30 to 60 °C [2]. The Arrhenius equation reads

$$\ln k_p\,(\mathrm{l\,mol^{-1}\,s^{-1}}) = 18.20 - 4295(T^{-1}\,(\mathrm{K^{-1}})), \qquad (30\,^{\circ}\mathrm{C} \le \theta \le 60\,^{\circ}\mathrm{C}) \tag{7}$$

with $A = 8.05 \times 10^7$ l mol^{-1} s^{-1} and $E_A = 35.7$ kJ mol^{-1}.

2.2.5.3. Ethene. The propagation rate coefficient for the high-pressure ethene polymerization has not been determined by PLP–SEC so far. The SP–PLP technique (Section 3) has, however, been successfully applied to derive both k_p and k_t [77,78]. The following equation gives the pressure and temperature dependence of k_p:

$$\ln k_p\,(\mathrm{l\,mol^{-1}\,s^{-1}}) = 16.75 - (4126 + 0.33p\,(\mathrm{bar}))(T^{-1}\,(\mathrm{K^{-1}})),$$
$$(190\,^{\circ}\mathrm{C} \le \theta \le 230\,^{\circ}\mathrm{C}) \text{ and } (1950\ \mathrm{bar} \le p \le 2900\ \mathrm{bar}) \tag{8}$$

Eq. (8) holds for monomer conversions up to at least 40%. The activation energy is $E_A = 34.3$ kJ mol^{-1}. The high value of E_A is due to the fact that the ethene double bond is not activated.

2.2.6. Miscellaneous

2.2.6.1. Methacrylonitrile. The propagation reaction of methacrylonitrile was studied between 10 and 60 °C [50]. Reactions carried out in bulk and in solutions of toluene and benzene did not show any

Table 7
Overview on propagation rate coefficients at 30 °C, k_p (30 °C), Arrhenius parameters, A and E_A, and activation volumes, $\Delta V^{\#}$, for various monomers

Monomer	k_p (30 °C) (l mol^{-1} s^{-1})	$A \times 10^7$ (l mol^{-1} s^{-1})	E_A (kJ mol^{-1})	$\Delta V^{\#}$ (cm^3 mol^{-1})
Ethene[a]	16[b]	1.88	34.3[c]	−27
1,3-Butadiene	57	8.05	35.7	–
Styrene	106	4.3	32.5	−11.7
Methacrylonitrile	20	0.27	29.7	–
Chloroprene	500	2.0	26.6	–
Dimethyl itaconate	11	0.020	24.9	–
Methacrylates (MMA–HPMA)	390 to 900	0.19 to 0.60	20.2 to 22.9	−16
Vinyl esters (VEOVA, VAc)	3000 to 4000	1.3 to 2.0	20.5 to 22.2	−10.7
Acrylates (MA–DA)	15 000 to 24 000	1.6 to 1.9	17.4	−11.7

[a] k_p derived from SP–PLP experiments.
[b] Formal ambient pressure value (see text).
[c] E_A determined for pressures between 1950 and 2900 bar.

solvent effect. Thus, the entire data set was fit by one Arrhenius expression:

$$\ln k_p \text{ (l mol}^{-1}\text{ s}^{-1}) = 14.81 - 3572(T^{-1}\text{ (K}^{-1})) \quad (9)$$

Eq. (9) is associated with a pre-exponential factor A of 2.69×10^6 l mol^{-1} s^{-1} and an activation energy of 29.7 kJ mol^{-1}. This A value is close to the ones for monomers of the methacrylate family (Tables 3 and 4).

2.2.6.2. Itaconates. PLP–SEC experiments in bulk were performed for dimethyl itaconate (DMI) in a temperature range from 20 to 50 °C [66]. The temperature dependence of k_p is described by the following equation:

$$\ln k_p \text{ (l mol}^{-1}\text{ s}^{-1}) = 12.28 - 2995(T^{-1}\text{ (K}^{-1})) \qquad (20\,^{\circ}\text{C} \le \theta \le 50\,^{\circ}\text{C}) \quad (10)$$

The k_p value at 50 °C is 20 l mol^{-1} s^{-1}. This value is one of the smallest k_ps determined so far by PLP–SEC. Only for MAN has a similarly low value been deduced.

2.2.7. Comparison of monomer families

The Arrhenius parameters A and E_A as well as k_p at 30 °C of the monomers discussed in Sections 2.2.1–2.2.5 are summarized in Table 7. As far as they are available, activation volumes are also included.

The monomers in Table 7 are given in the order of decreasing activation energies. The activation energies determined for the acrylates and the methacrylates are around 17.5 and 22 kJ mol^{-1}, respectively. The activation energies for styrene, vinyl acetate, butadiene, and dimethyl itaconate are E_A = 32.5, 20, 35.7, and 24.9 kJ mol^{-1}, respectively.

Fig. 5 illustrates the temperature dependence of k_p for a large series of monomers. The lower and upper lines for the methacrylates represent k_p of MMA and DMA, respectively. The lower and upper lines in the acrylate family correspond to MA and DA, respectively. The dashed parts of the log k_p lines

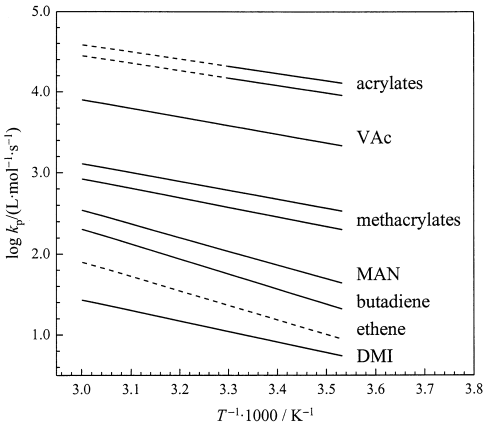

Fig. 5. Temperature dependence of k_p at ambient pressure for a series of monomers. The upper and lower lines for the acrylates and methacrylates refer to the dodecyl and the methyl ester, respectively. The dashed lines indicate extrapolated data.

for the acrylates account for the fact that k_p values in these ranges have not been determined experimentally. k_p of ethene is also represented by a dashed line, since ambient pressure values for (gaseous) ethene are not available. The data in Fig. 5 is the estimated ethene k_p for 51 bar, which is approximately the critical pressure of ethene. It is evident that the variation of k_p within the family of the acrylates and within the family of the methacrylates is very small as compared to the observed difference in k_p, of more than four orders of magnitude, e.g. between DMI and DA. Fig. 5 visualizes that with the exception of DMI, the activation energies are highest for monomers with low k_p values.

Fig. 6 shows the pressure dependence of k_p for acrylates, methacrylates, VAc and styrene. Again, acrylates and methacrylates are represented by the limiting methyl and dodecyl ester systems. It is clearly seen from Fig. 6 that the pressure dependence of k_p for the methacrylates is more pronounced than for the other monomers. This finding is explained by the higher steric demand of the transition state

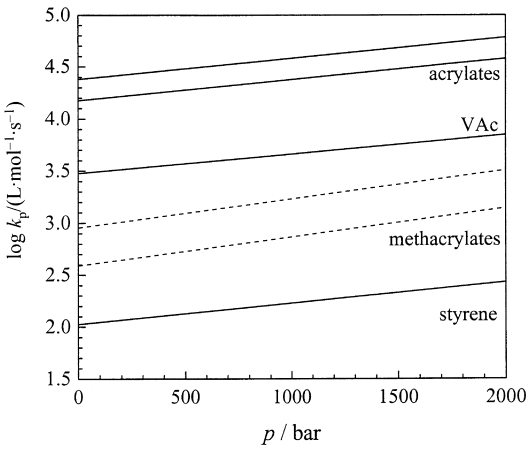

Fig. 6. Pressure dependence of k_p at 30 °C for a series of monomers. The upper and lower lines for the acrylates and methacrylates refer to the dodecyl and the methyl ester, respectively.

in methacrylate propagation [79]. The steric demand of the transition state is very similar for the other monomers in Fig. 6. Each of these monomers has an α-hydrogen atom at the free-radical reaction site. The transition state thus is less congested as with the methacrylates. The activation volume is $-16\,\mathrm{cm^3\,mol^{-1}}$ for the methacrylates and between -10.7 and $-11.7\,\mathrm{cm^3\,mol^{-1}}$ for the other monomers.

2.3. Propagation rate coefficients in copolymerizations

The essential problem of measuring reliable copolymerization propagation rate coefficients, $k_{p,copo}$, by PLP–SEC relates to the requirement of SEC-calibration for each experimental copolymer composition. As has been discussed in Section 2.1.2, this may be achieved via absolute calibration or by applying universal calibration, which is the most frequently used method. In rare cases such as styrene–MMA copolymerization, it has been found that the Mark–Houwink constants required for SEC-calibration may be established by linear interpolation between the Mark–Houwink constants of the associated homopolymers [80].

2.3.1. Copolymerization models

A comprehensive survey on the mechanism of propagation steps in free-radical copolymerization has recently been provided by Coote and Davis [81]. For a brief overview on the models used to describe copolymerization propagation rate coefficients, $k_{p,copo}$, the reader is referred to Refs. [82,83]. Only a short description will be given here.

The simplest model to represent $k_{p,copo}$ is the 'terminal' model (TM) in which it is assumed that propagation reactivity is solely determined by the monomer molecule and by the terminal unit at the free-radical chain end. The general expression for $k_{p,copo}$ reads

$$k_{p,copo} = \frac{\bar{r}_1 f_1^2 + 2 f_1 f_2 + \bar{r}_2 f_2^2}{(\bar{r}_1 f_1 / \bar{k}_{p11}) + (\bar{r}_2 f_2 / \bar{k}_{p22})} \tag{11}$$

with f_i being the mole fraction of monomer i in the feed and $\bar{r}_i = r_i$, the reactivity ratio, defined as $r_i = k_{pii}/k_{pij}$, where k_{pij} refers to the addition of monomer j to a free-radical terminating in a unit derived from monomer i.

In their pioneering work, Fukuda et al. [84] demonstrated that the terminal model mostly fails to describe copolymer compositions and propagation rates simultaneously. On the other hand, as has been shown by Schweer [85], the terminal model allows for adequate separate fits of copolymer composition and of $k_{p,copo}$ (Eq. (11)) as a function of monomer feed composition. This procedure is, however, associated with the unfavorable situation of providing two sets of 'terminal' reactivity ratios for a single system. Fukuda et al. [84] recommended the use of 'penultimate' models in which both the terminal and the penultimate units at the free-radical chain end are assumed to affect propagation kinetics. The penultimate models, in addition to the terminal unit, also specify the monomeric unit in penultimate position to the free-radical site. This extension increases the number of propagation rate coefficients, k_{pijk}, to eight. By rationing individual k_{pijk}s, four reactivity ratios, r_{ij}, and two radical reactivity ratios, s_i, are obtained:

$$r_{ii} = \frac{k_{piii}}{k_{piij}}; \qquad r_{ij} = \frac{k_{piij}}{k_{piji}}; \qquad s_i = \frac{k_{pjii}}{k_{piii}} \tag{12}$$

As has been shown by Fukuda et al. [84], the terminal and penultimate reactivity ratios and propagation rate coefficients are related by the following set of expressions:

$$\bar{r}_i = r_{ji}\frac{r_{ii}f_i + f_j}{r_{ji}f_i + f_j} \tag{13}$$

$$\bar{k}_{\mathrm{p}ii} = k_{\mathrm{p}iii}\frac{r_{ii}f_i + f_j}{r_{ii}f_i + f_j/s_i} \tag{14}$$

Two such models have been considered, the 'implicit penultimate unit effect (IPUE)' [84] and the 'explicit penultimate unit effect (EPUE)' [86] model. Aspects of both models are detailed in Refs. [81,83] and will not be reiterated here. The IPUE model assumes that both terminal and penultimate units affect free-radical reactivity but selectivity is only determined by the terminal unit. Most of the systems that have been studied so far are adequately described by the IPUE model in which it is assumed that $r_{11} = r_{21} = r_1$ and $r_{22} = r_{12} = r_2$. The IPUE model thus contains four parameters: r_1, r_2, s_1, and s_2. It has been successfully applied toward simultaneously fitting copolymer composition and $k_{\mathrm{p,copo}}$ as a function of monomer feed composition.

Only for a very few systems has it appeared necessary to consider the full penultimate scheme with six parameters: r_{11}, r_{21}, r_{22}, r_{12}, s_1, and s_2. Within the EPUE model, it is assumed that the terminal and penultimate units of the free radical affect both reactivity and selectivity. In Ref. [81], the discrimination between IPUE and EPUE models is addressed in great detail and evidence from various types of experiments and from molecular orbital calculations of reaction barriers and frequency factors of associated reactions of small free radicals has been included into the discussion.

2.3.2. Experimental data for binary copolymerizations

The binary copolymerization systems studied by PLP–SEC so far are given in Table 8. The table lists temperature θ, the best suited model, homopropagation coefficients $k_{(i)ii}$ of both monomers, reactivity ratios, and—if reported—radical reactivities.

Table 8 indicates that most systems are represented best by the IPUE model. Only for a few special systems, does the terminal model provide a good description of both $k_{\mathrm{p,copo}}$ and copolymer composition. The first such system is the copolymerization of MMA with perdeuterated MMA [87]. The two reactivity ratios are found to be unity. It is not overly surprising that the terminal model nicely works in a copolymerization system where the two monomers are practically identical. The same holds true for copolymerizations of styrene with a substituted styrene or for copolymerizations of two substituted styrenes [88–90]. With substituents in the *para*-position, steric hindrance or shielding of the radical site is not expected to occur, since small groups such as methoxy or Cl are introduced. Thus, the observed variation of $k_{\mathrm{p,copo}}$ is due to the change in radical stability/monomer reactivity, which in many cases is adequately represented by considering the terminal model.

$k_{\mathrm{p,copo}}$ of systems containing an acrylate and a methacrylate monomer have recently been studied [83,91]. With MMA and BA or MA and DMA being the copolymerizing monomers, $k_{\mathrm{p,copo}}$ and copolymer compositions are adequately described by the IPUE model. The IPUE and also the EPUE model, however, fail to simultaneously represent the $k_{\mathrm{p,copo}}$ and copolymer composition data for the DA–MMA and the DA–DMA system, but $k_{\mathrm{p,copo}}$ of the two DA-containing systems is well fitted by the terminal model [91]. These findings indicate that with DA being one of the comonomers, individual

Table 8
Binary copolymerization systems studied by PLP–SEC. The table lists temperature θ, the best suited model, homopropagation coefficients $k_{(i)ii}$ of both monomers, reactivity ratios, and—if reported—radical reactivities, see text for further details

M_1	M_2	Model	θ (°C)	$k_{(1)11}$	$k_{(2)22}$	$\bar{r}_1$	$\bar{r}_2$	s_1	s_2	Reference
MMA	d-MMA[a]	TM	25	270	342	1	1	–	–	[87]
S	MeS	TM	27.7	112	0.62[b]	0.07	0.92	–	–	[88]
MOS	S	TM	25[c]	52	86	0.82	1.12	–	–	[89]
Cl–S	S	IPUE	40	197	160	1.1	0.543	0.819	1.07	[90]
Cl–S	MOS	TM	40[c]	175	94	1.04	0.412	–	–	[90]
S	MMA	IPUE	25	89.8	299.2	0.523	0.46	0.30	0.80	[181]
S	MMA	IPUE	25	77.5	294	0.472	0.454	0.466	0.175	[182]
S	MMA	IPUE	50	246	631	0.48	0.42	0.31	2.1	[93]
S	MMA	IPUE	47.5	215	576	0.489	0.493	0.31	0.66	[183]
S	EMA	IPUE	25	78	258	0.62	0.35	0.62	0.21	[184]
S	EMA	IPUE	55	249	589	0.62	0.35	0.45	0.22	[184]
S	BMA	IPUE	25	78	274	0.72	0.45	0.56	0.63	[184]
S	BMA	IPUE	55	249	656	0.72	0.45	0.50	0.67	[184]
S	DMA	IPUE	25[c]	78	776	0.57	0.45	0.33	0.26	[184]
S	MEA	TM	30	110	20[b]	0.224	0.782	–	–	[82]
MOS	MMA	IPUE	25[c]	52	300	0.32	0.29	0.36	0.60	[89]
BA	MMA	IPUE[d]	20	11 750[e]	294	0.40	2.15	0.43	1.98	[91]
BA	MMA	IPUE	60	33 870[e]	847	0.40	2.15	0.43	1.98	[83]
BA	MMA	IPUE	40[f]	35 541	1017	0.36	2.55	Ind.	1.9	[91]
MA	DMA	IPUE	40[f]	28 567	1607	0.23	2.57	0.05	1.9	[91]
DA	MMA	TM[g]	40[f]	39 813	1017	0.53	0.88	–	–	[91]
DA	DMA	TM[g]	40[f]	39 813	1607	0.21	0.88	–	–	[91]

[a] Perdeuterated MMA.
[b] k_p for MEA cannot be determined due to depropagation; the given value is derived from the terminal model fit to the experimental data.
[c] Polymerization in solution of toluene.
[d] IPUE fit to the combined data set (20 and 60 °C) of $k_{p,copo}/k_p$ (MMA).
[e] k_p for BA is estimated to be 40 times higher than k_p for MMA.
[f] 1000 bar.
[g] Terminal model fit to only the $k_{p,copo}$ data.

propagation rate coefficients are not adequately described by the consideration of only the terminal and penultimate units at the free-radical chain end. It is suggested that the free-radical reactivity in these systems may be influenced by pen-penultimate unit effects. The TM being applied to monomer and copolymer composition data considers only ratios of individual propagation rate coefficients of free radicals with the same penultimate unit and thereby seems to eliminate most of the impact of the penultimate units. For this reason, the widely used 'terminal model' reactivity ratios resulting from the Lewis–Mayo equation are reasonable and give meaningful kinetic quantities although penultimate effects on the individual propagation rate coefficients are undoubtedly operative. For a detailed discussion the reader is referred to Ref. [91].

With respect to the *s*-values given in Table 8, it should be noted that they are highly uncertain. As has been discussed previously [83,91–93], the *s*-value referring to the addition of the monomer with the higher k_p value is often only poorly determined: for the acrylate–methacrylate systems $\bar{r}_1\bar{r}_2$ is close to

unity, under which conditions s_1 and s_2 are strongly correlated. Secondly, if $\bar{r}_1/k_{p11} \gg \bar{r}_2/k_{p22}$ (1: methacrylate, 2: acrylate), the denominator in Eq. (11) is hardly affected by the second term which prevents reliable estimates for s_2. This is one of the reasons why trends in s-values are difficult to establish and conclusions on $k_{p,copo}$ modeling are scarce. Nevertheless, listed s-values may be used to estimate $k_{p,copo}$ as a function of monomer feed composition, e.g. for calculating copolymerization rate. This procedure just reverses the process by which the r_i and s_i values have been derived and thus is less sensitive to the validity of the underlying model.

In addition to the binary systems, two ternary copolymerizations have been studied via the PLP–SEC technique: styrene–MMA–MA [94] and *p*-methoxystyrene–styrene–MMA [95].

Besides the above mentioned terminal model and the penultimate unit models, Harwood suggested the bootstrap model [96] to explain observations from copolymerizations in solution. Especially for systems involving polar monomers, the partitioning of monomers between solvent and the domain of the growing polymer radical should occur. Due to solubility aspects, the monomer feed composition in the vicinity of the propagating chain-end may be different from the bulk monomer feed composition.

2.4. Solvent influence on propagation rate

It is well-known that a solvent may significantly affect the diffusion-controlled termination reaction (Section 3.6) and thus k_t may be strongly altered. For chemically controlled reactions, e.g. propagation in free-radical polymerizations, no such strong solvent effect is expected. However, as has been reported, moderate variations of k_p result upon the addition of a solvent. Arguments for a solvent dependence of propagation rate coefficients encompass influences originating from (1) polarity, (2) interaction between polymer and solvent, (3) interaction between monomer and solvent, and (4) the complexation between the propagating free radical and the solvent [97]. Other authors suggest that local monomer concentration effects may play a major role [96,98,99].

Early PLP–SEC investigations into the influence of solvents on the propagation rate coefficient in free-radical homopolymerizations of MMA and styrene suggested that k_p is almost invariant toward the type and the concentration of the solvent. Within several of these studies, however, solvents have been used which are not too dissimilar from the monomer. Recently, more extended studies showed a significant solvent effect on k_p with a few conventional solvents and, in particular, with fluid and supercritical carbon dioxide ($scCO_2$). This data will be summarized and discussed in Sections 2.4.1 and 2.4.2.

2.4.1. Polymerizations in organic solvents

As for bulk polymerizations, the most widely studied monomers in solution polymerizations are MMA and styrene. Olaj and Schnöll-Bitai [38] reported k_p data at 25 °C for MMA and styrene homo- and copolymerizations in a large number of solvents. For styrene, k_p values are up to 12% below the corresponding bulk value of k_p, $k_{p,bulk}$. Only for polymerizations in cyclohexane was a larger change observed: k_p is increased by 21% as compared to the bulk value. In MMA polymerizations a decrease of k_p of at most 14% is observed for all solvents with the exception of DMF, for which k_p is 7% higher than $k_{p,bulk}$. The copolymerization experiments showed an increase of k_p in DMF and in cyclohexane of 15 and 25%, respectively. All other reported $k_{p,copo}$ data are within ±6% of the bulk value. This is within the limits of experimental accuracy for k_p determination via PLP–SEC. In summary, mostly minor solvent

effects are found. The enhancement of k_p in the presence of the poor solvent cyclohexane was interpreted as being due to local monomer concentrations being different from overall concentrations [38].

Investigations into solvent effects on k_p for styrene and MMA homopolymerizations in benzyl alcohol by O'Driscoll et al. [39] and Zammit et al. [34] indicated a strong increase of k_p with solvent concentration. Compared to the corresponding bulk values, k_p of MMA increases by up to 74% and k_p of styrene by up to 60% depending on the temperature. These effects are interpreted as being due to complex formation between the free-radical chain ends and solvent molecules. Zammit et al. [34] reported a solvent effect on k_p for MMA and styrene homopolymerizations in six additional solvents. For five solvents (diethyl malonate, diethyl phthalate, bromobenzene, dimethyl sulfoxide, *N*-methyl pyrrolidinone) an increase in k_p was found as compared to $k_{p,bulk}$. An enhancement of k_p by 63% is seen for MMA polymerizations in dimethyl sulfoxide (DMSO) at 26.5 °C. Polymerizations in chlorobenzene under otherwise identical conditions resulted in a slight decrease of k_p by about 7%. The latter variation is within the typical accuracy of ±10% estimated for k_p data from PLP–SEC.

The propagation reaction of ethyl α-hydroxymethacrylate has been studied in a wide variety of solvents: benzene, chlorobenzene, chloroform, cyclohexane, dichloromethane, ethanol, ethyl acetate, ethyl benzene, pentan-1-ol, propan-1-ol, THF, toluene, and xylene [65]. In these solution polymerizations, the general trend of a decrease in k_p with increasing dielectric constant of the solvent is observed. At monomer concentrations of around 2 mol l^{-1} and 25 °C, k_p decreases from around 1800 l mol^{-1} s^{-1} in xylene to around 600 l mol^{-1} s^{-1} in THF and in ethanol. In addition, the temperature dependence of k_p has been investigated for three monomer concentrations in THF, toluene, and ethanol. The strongest variation of activation energy with monomer concentration is observed for reactions in THF: E_A increases from 16.3 to 23.5 kJ mol^{-1} for monomer/solvent ratios of 3:1 and 1:3, respectively. In ethanol, E_A increases from 14.6 to 20.7 kJ mol^{-1} and in toluene from 16.1 to 19.8 kJ mol^{-1} for monomer/solvent ratios of 3:1 and 1:3, respectively. In case of high dilution, E_A even approaches values that are typical for methacrylate k_p, whereas at higher monomer concentrations, E_A is significantly lower, comparable to acrylate E_A. The solvents affect both the activation energy and the pre-exponential factor. The authors [65] assume that the interactions between the monomer and the propagating radical in the transition state are modified by the action of solvent.

An investigation [40] into solution polymerizations of styrene in *N*-dimethyl formamide (DMF) and acetonitrile revealed a decrease of k_p by up to 25 and 15%, respectively, in good agreement with the k_p data for styrene polymerizations in DMF reported in Ref. [38]. The observed reduction of k_p is also interpreted as being due to direct interaction of the solvent with the transition structure of the propagation step [40].

In contrast to the above summarized results for solution polymerizations of ethyl α-hydroxymethacrylate [65], the k_p data for styrene and MMA homopolymerizations in various solvents reported by Olaj and Schnöll-Bitai do not show any correlation of k_p with the dielectric constant [38]. Moreover, the k_p data for homopolymerizations of MMA and styrene in benzyl alcohol and in NMP show the opposite trend: k_p is increased in the presence of solvents, which have higher dielectric constants than the monomers [34,39].

As part of a study into depropagation kinetics, the solvent influence on k_p for methacrylate polymerizations has been studied for reactions in 2-heptanone and in *n*-octyl acetate at monomer concentrations of 25 vol% [48]. For BMA only a slight increase of k_p, by about 10%, has been observed for polymerization in 2-heptanone at 90 °C, whereas no change in k_p was seen at 30 °C. For DMA and CHMA polymerizations in 2-heptanone and in *n*-octyl acetate, a stronger solvent effect was found: k_p values of

DMA are reduced by 26% at 90 °C and by 14% at 30 °C. For CHMA, the solvent influence is the largest at 30 °C, where a reduction of 40% is found. No significant change of k_p occurs at 90 °C. These relatively small variations of k_p in the presence of 2-heptanone and *n*-octyl acetate are not expected to be due to specific interactions between solvent and monomer or between solvent and propagating radical. The variations are supposed to be due to the local monomer concentrations, $c_{M,loc}$, within the vicinity of the free-radical chain end being different from overall monomer concentration, c_M. One way to distinguish whether effects result from local monomer concentration or from a modification of interactions in the transition state is by monitoring the temperature dependence of k_p. In the latter case, $E_A(k_p)$ should be affected, whereas $E_A(k_p)$ is not influenced, if only the effective (local) monomer concentration is varied. A more detailed discussion of aspects associated with local monomer concentration will now be given.

2.4.2. Polymerizations in solutions of fluid CO_2

In addition to liquid solvents such as water or conventional organic solvents, fluid CO_2 has been chosen as a solvent for free-radical polymerization. Besides being an attractive new solvent for technical applications, fluid and, in particular, supercritical CO_2 ($scCO_2$) is also of interest with respect to mechanistic studies. Especially for studies into acrylate k_p, the use of $scCO_2$ might be beneficial, as CO_2 does not take part in chain-transfer reactions [100]. Further, CO_2 is not expected to form complexes with neither the monomer nor with the macroradical or with the polymer. In addition, using CO_2 as the solvent medium allows for investigations into the influence of solvent quality and thus chain geometry on the propagation reaction. It is known that CO_2 is a rather poor solvent for polystyrene, polymethacrylates and polyacrylates [101]. (Note: although CO_2 is a poor solvent for the polymers under investigation, PLP–SEC experiments at low degrees of monomer conversion may be carried out in a homogeneous phase.)

The first study into k_p in CO_2 was by van Herk et al. [36]. These authors reported k_p data for MMA and styrene at 65 °C and 180 bar. At these conditions, no influence of CO_2 on k_p was observed. An additional study into the temperature dependence of k_p for MMA polymerization in $scCO_2$ at 180 bar also showed no effect of CO_2 on k_p within experimental uncertainty [43].

However, PLP–SEC investigations [44] into the variation of k_p with CO_2 concentration for homopolymerizations of MMA, at 30 °C/1000 bar, and BA, at −1 °C/1000 bar as well as at 11 °C/200 bar, showed a significant reduction of k_p compared to $k_{p,bulk}$. This is demonstrated in Fig. 7. In going from bulk polymerization to solution polymerization with 60 wt% of CO_2, k_p is reduced by 40% for both monomers. The discrepancy to the previous results for MMA polymerizations [36,43] is supposed to be due to molecular weight, which has been much higher in the experiments described in Ref. [44].

Investigations into the temperature and pressure dependence of k_p for BA polymerizations in CO_2 showed that k_p is always near 40% below the corresponding $k_{p,bulk}$ value. The activation energies and activation volumes [57] are the same for the bulk and solution (in $scCO_2$) polymerizations, which suggests that the CO_2 influence on k_p from PLP–SEC is not or not entirely a kinetic effect resulting from changes in the activation barrier or in the steric requirements of the activated state.

Inspection of Eq. (1) indicates that only the product $c_M k_p$ is obtained from the experimentally accessible quantities L_1 (from SEC) and t_0 (from the inverse of the laser pulse repetition rate). Thus, solvent effects on the propagation rate may be due to changes of k_p, of c_M, or to changes to both these quantities. If one assumes k_p to be invariant with CO_2 content, the experimental findings may reflect a deviation of local monomer concentration at the free-radical site from the overall monomer concentration. This deviation appears to be different for bulk and solution polymerizations. This effect may be due to

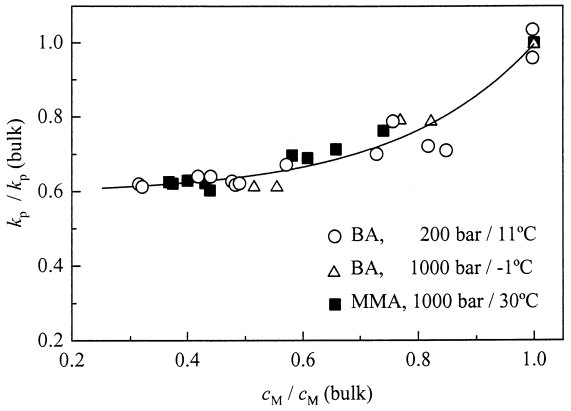

Fig. 7. Variation of the relative propagation rate coefficient $k_p/k_{p,bulk}$ with relative monomer concentration $c_M/c_{M,bulk}$ for MMA (filled marker) and BA (open marker) polymerizations in CO_2. Reproduced with permission from Macromol Chem Phys 1998;199:1209. © 1998 Wiley–VCH [44].

shielding of the free-radical chain-end [102], or to *intra*segmental interactions within the propagating radical. This view is in agreement with discussions on preferential solvation by Kuchanov and Russo [103] and Kratochvil et al. [99]. The latter authors suggest that solvent quality determines local monomer concentrations. Explanations for the solvent influence on copolymer composition by Harwood [96] and Semchikov [98] are also based on arguments of this kind.

Interestingly, corresponding studies into styrene polymerizations revealed that k_p values in bulk and in solutions of $scCO_2$ are identical [37]. As the solvent quality of CO_2 for polystyrene is poor, the insensitivity of k_p toward the CO_2 environment suggests that solvent quality arguments alone cannot explain variations of k_p induced by CO_2.

Further investigations were carried into k_p for homopolymerizations of MA and DA in 40 wt% CO_2. A significant reduction of k_p as compared to $k_{p,bulk}$ is seen. The reduction is larger for MA, by 40%, than for DA, by 25% [55]. As for BA, the activation volumes and activation energies are identical for reactions in CO_2 and in bulk.

The experimental findings may be understood by considering a competition of the interaction of polymer segments with (a) other polymer segments of the same macroradical and with (b) solvent molecules, monomer and CO_2 in this particular case [55,57]. The type of interactions between CO_2 and polymer segments carrying a polar group, e.g. PMMA has been investigated by Kazarian et al. [104,105]. Strong *intra*segmental interactions may reduce the local monomer concentration. In polystyrene, where dipolar interactions are absent, no reduction of local monomer concentration as compared to overall concentration is expected. Interactions of polar segments should be particularly pronounced in MA, and should be important in MMA and in BA. The smaller effect observed for DA, where k_p in solution is only by 25% below $k_{p,bulk}$, may be understood by shielding effects of the large ester chain, by which the extent of *intra*segmental interaction is diminished. According to these arguments, CO_2 should also decrease k_p for vinyl acetate polymerization. k_p values for VAc polymerizations in bulk and in solution of CO_2 are, however, the same [62]. The reason behind this observation probably is that CO_2 favorably interacts with the VAc-segments [106], which is reflected in a relatively good solubility of poly(vinyl acetate) (PVAc) in $scCO_2$. As compared to PVAc, the isomeric poly(methyl acrylate) has a

much lower solubility in $scCO_2$. This observation is consistent with $c_{M,loc}$ being smaller in MA polymerization as compared to VAc polymerizations, where $c_{M,loc}$ is close to the overall concentration. It goes without saying that the same kind of effects is operative for other solution polymerizations.

In summary, the apparent solution k_p, which results from the analysis of PLP–SEC data by identifying c_M with overall monomer concentration, may be different from $k_{p,bulk}$ in cases where polar *inter*segmental interactions are operative and, at the same time, the interactions between solvent molecules and polymer segments are clearly different from the ones between monomer molecules and polymer segments. Depending on solvent quality, local monomer concentrations may decrease or increase.

The arguments concerning local monomer concentration assume that k_p in solution and in bulk is not significantly different. This assumption seems to be fulfilled in systems where activation energies and activation volumes are identical for bulk and solution polymerizations.

2.4.3. Water-soluble monomers: acrylic acid, methacrylic acid, and N-isopropylacrylamide

PLP–SEC investigations into polymerizations in aqueous phase have been carried out for methacrylic acid (MAA), acrylic acid (AA), and *N*-isopropylacrylamide (NIPAM). In addition, the polymerization of MAA has been studied in several organic solvents. The determination of k_p for these monomers is not only a challenge due to the difficulty in finding proper PLP conditions. The analysis of the polymeric product by SEC poses quite some problems: poly(acrylic acid) (PAA) and poly(methacrylic acid) (PMAA) cannot be directly analyzed via conventional SEC with THF as the eluent. Therefore, two approaches have recently been pursued: (i) esterification of PAA to PMA and of PMAA to PMMA, and subsequent MWD analysis via SEC with THF [51,52]. (ii) Direct analysis of PAA and PMAA with an SEC set-up operated with an aqueous phase as the eluent [59]. Poly(NIPAM) samples were analyzed using a special THF-based SEC technique [58,107].

The most extended data set is available for k_p of MAA. The reactions were carried out in bulk and in solution of water, DMSO, methanol, THF, toluene, acetic acid, and 2-propapanol. With the exception of polymerizations carried out in aqueous phase, k_p values did not show a strong dependence on the type and concentration of the solvent. MAA polymerizations in water showed a strong enhancement of k_p with decreasing monomer concentration: e.g. k_p at 25 °C increases from 605 to 3922 l mol^{-1} s^{-1} upon lowering the concentration from 9.34 mol l^{-1} to 1.71 mol l^{-1} s^{-1}. Table 9 gives k_p values and Arrhenius parameters for MAA polymerizations at 60 °C in solution of water, methanol and DMSO. In addition, k_p data at 60 °C for MAA polymerizations in toluene, THF, HAc, and 2-propanol are listed. The activation energies, $E_A(k_p)$, obtained for the different solvents are in the range from 15.3 to 21.4 kJ mol^{-1}. Comparison of k_p values determined at 60 °C, however, does not show a clear trend.

Acrylic acid polymerizations were carried out at various acid concentrations in water. The studies revealed a decrease of k_p with increasing monomer content [59]. The temperature variation of k_p has been studied for two monomer concentrations, 20 and 40 wt% AA so far. The resulting Arrhenius equations read:

$$20\ \text{wt\% AA} \quad \ln k_p\ (\text{l mol}^{-1}\ \text{s}^{-1}) = 16.34 - 1443(T^{-1}\ (\text{K}^{-1})) \quad (2.3\ ^\circ\text{C} \le \theta \le 25.0\ ^\circ\text{C}) \quad (15)$$

$$40\ \text{wt\% AA} \quad \ln k_p\ (\text{l mol}^{-1}\ \text{s}^{-1}) = 15.99 - 1467(T^{-1}\ (\text{K}^{-1})) \quad (2.3\ ^\circ\text{C} \le \theta \le 28.5\ ^\circ\text{C}) \quad (16)$$

The pre-exponential factors are 12.5×10^6 and 8.80×10^6 l mol^{-1} s^{-1} at 20 and 40 wt% acrylic acid in

Table 9
Arrhenius parameters, A and E_A, and propagation rate coefficients at 60 °C, k_p (60 °C), for methacrylic acid polymerizations in solution of the listed solvents; Θ interval indicates the temperature range in which the data has been measured

Solvent	$A \times 10^6$ (l mol^{-1} s^{-1})	E_A (kJ mol^{-1})	k_p (60 °C) (l mol^{-1} s^{-1})	Θ Interval (°C)	Reference
Water[a]	1.72	15.3	6864	18–89	[52]
MeOH[b]	1.63	20.5	995	22–60	[52]
MeOH[c]	0.603	17.7	1012	20–60	[51]
DMSO[b]	3.4	21.4	1500	23–90	[52]
THF[c]	–	–	862	–	[51]
HAc[c]	–	–	1040	–	[51]
2-Propanol[c]	–	–	977	–	[51]
Toluene[c]	–	–	1226	–	[51]
Bulk	–	–	1179	–	[51]

[a] 15 wt% MAA.
[b] 30 wt% MAA.
[c] 33 vol% MAA.

water, respectively. For both monomer concentrations, an activation energy of around 12 kJ mol^{-1} is obtained. This value is below the activation energy of 17 kJ mol^{-1} observed in acrylate polymerizations. A similar trend is seen in comparing MAA solution polymerizations in water with MMA bulk polymerizations. As can be seen from Table 9, the value for $E_A(k_p)$ for aqueous MAA polymerization is 15.3 kJ mol^{-1}, which has to be compared with $E_A(k_p) = 22$ kJ mol^{-1} for the methacrylates (Tables 3 and 4). It should be noted that the activation energies for MAA polymerizations in methanol and in DMSO are closer to the typical values for methacrylate polymerizations.

For an aqueous solution containing 20 wt% AA, Lacík et al. [59] determined a k_p value of 100 000 l mol^{-1} s^{-1} at 25 °C. This value, which has been determined by aqueous phase SEC, is significantly higher than what would be expected from the data reported by Kuchta et al. [52]. The latter authors used the esterification route. The discrepancy may indicate that the esterification procedure is associated with some structural changes of the polymer. Such changes are not expected to occur in the esterification of PMAA samples [59,108,109]. As a consequence, the quality of reported k_p(MAA) data should not be affected by the esterification procedure.

Aqueous phase polymerizations of NIPAM result in k_p values, which also show a pronounced dependence on monomer concentration: k_p increases significantly with decreasing monomer concentration. For example, for NIPAM concentrations of 0.08 and 0.2 mol l^{-1} PLP–SEC experiments at 20 °C yield k_p values around 70 000 and 27 000 l mol^{-1} s^{-1}, respectively.

2.5. Special applications of PLP–SEC

2.5.1. Chain-transfer rate coefficients

PLP–SEC experiments are not restricted toward the determination of propagation rate coefficients. If the reaction conditions are suitably chosen, PLP–SEC may also provide easy access to transfer rate coefficients, k_{tr}, preferably of k_{tr} for chain-transfer agents (CTA). As outlined in Section 2.1.1, the determination of k_p requires reaction conditions under which chain-transfer reactions contribute only to a minor extent to the chain-stopping events and thus assure the validity of a linear

correlation of the number of propagation steps between two successive laser pulses with the time between these pulses. Depending on the monomer under investigation, high laser pulse repetition rates may be necessary in order to suppress the influence of chain-transfer (compare Section 2.2.3 on k_p for acrylates). To derive k_{tr} from PLP–SEC, chain-transfer has to be the major chain-stopping mechanism. This may be achieved by increasing the time between laser pulses and choosing a low initiator concentration, which makes termination events less probable. As has been outlined by Hutchinson et al. [16] these reaction conditions are contrary to the conditions applied to derive k_p. Thus, PLP–SEC allows for the determination of either k_{tr} or k_p. Simultaneous estimation of k_{tr} and k_p is not feasible in a conventional PLP–SEC experiment, but may be achieved by choosing a special sequence of pulses (see below).

Combination of PLP with the chain-length distribution (CLD) method as introduced by Clay and Gilbert [110] is especially attractive for deducing k_{tr}. In this method the logarithm of the number MWD, $f(M)$, is plotted vs. M. In contrast to the Mayo method, which relies on number average molecular weight, M_N, derived from the complete polymer MWD, the CLD technique considers only a section of the MWD at intermediate molecular weights. Thus problems, that may arise from an incomplete separation of low molecular weight material, e.g. residual monomer, which affects M_N are excluded or are minimized. In addition, problems resulting from difficulties in the accurate analysis of the high-molecular-weight side of the MWD, due to a high-molecular-weight tail from spontaneous polymerization, due to a lack of reliable calibration standards for very high molecular weight, or due to branching of polymer as a result of transfer to polymer reactions, may be reduced or even eliminated. It has, however, been shown that under favorable conditions the Mayo- and the CLD-method yield the same results [111–113]. In these references, the proper selection of the molecular weight range for CLD analysis has been addressed in detail.

PLP–SEC experiments were carried out to derive k_{tr} for *n*-dodecyl mercaptan (DDM) being the CTA in methacrylate and styrene homopolymerizations [16]. It has been shown that the transfer constant $C_{tr} = k_{tr}/k_p$ of DDM is identical for MMA, EMA, and BMA. In addition, between 20 and 80 °C a temperature independent value of $k_{tr}/k_p = 0.68 \pm 0.02$ has been measured. In styrene polymerizations C_{tr} is by about a factor of 20 higher, $k_{tr}/k_p = (15.6 \pm 0.2)$.

Recently k_{tr} for DDM and for a cobalt(II)–porphyrin compound has been obtained in styrene and MMA homo- and copolymerizations in bulk and in solution of CO_2 [114–116].

As mentioned earlier, by selecting special pulse sequencing, k_{tr} and k_p may be derived from a single PLP–SEC experiment [117]. Fig. 8 illustrates the procedure. Three laser pulses separated by a time interval of $t = \nu_R^{-1}$ are followed by an extended dark time t_d. The packages of three pulses are sufficient to create the PLP structure I, shown on the RHS of Fig. 8, which allows to deduce k_p. Chain stopping during the dark time period, t_d, is dominated by chain transfer and yields the molecular weight contour II. Analysis of the high-molecular-weight range II, e.g. by the CLD method, yields the transfer rate coefficient. The feasibility of this so-called 'railroad' procedure for simultaneous k_p and transfer rate measurement has been shown by simulations [117].

2.5.2. Estimate of k_t from PLP–SEC experiments

In addition to the determination of k_p and k_{tr}, PLP–SEC may also be used to estimate the termination rate coefficient, k_t, from an inspection of the entire MWD. Several groups [6,7,12] pointed out that termination rate coefficients may be accessible from the MWD if additional information on overall polymerization rate (or on pulse induced free-radical concentration) is available. Olaj and Schnöll-Bitai

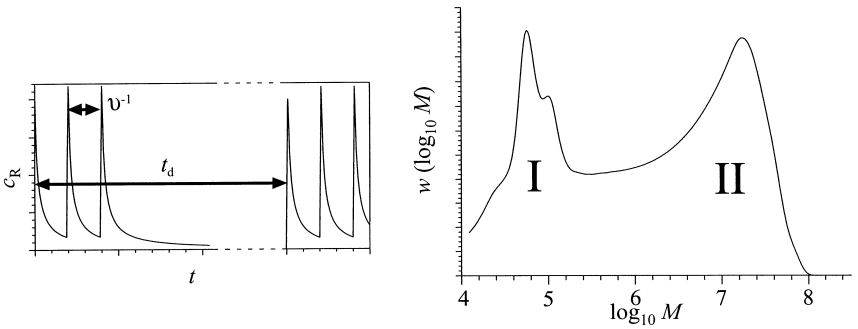

Fig. 8. Free-radical concentration, c_R, generated during a 'railroad' experiment (left) and associated SEC trace, $w(\log M)$ vs. $\log M$, of the polymeric product (right). I and II indicate molecular weight regimes being controlled by pulse laser termination and by chain transfer to monomer, respectively. Reproduced with permission from Macromol Theory Simul 1997;6:145. © 1997 Wiley–VCH [117].

[7] were the first to show, via styrene PLP-experiments, that k_t may be derived from Eq. (17) [118]

$$k_t = \frac{k_p^2 c_M^2 (3 - \delta)}{L_W r_0} \tag{17}$$

where δ is the relative contribution of disproportionation to overall termination, L_W is the weight average degree of polymerization, and r_0 is the overall polymerization rate (under pseudo-stationary conditions). It was shown that this relation is valid for arbitrary types of pseudo-stationary polymerization [6] as far as chain transfer is absent and k_t is independent of chain length. The method is reliable, and if L_W is calculated from an SEC trace, is almost insensitive toward axial broadening of SEC, as was confirmed by PREDICI® simulation [119]. Difficulties in k_t analysis via Eq. (17) may, however, result from spontaneous polymerization [118], from polymerization subsequent to PLP, and from chain-transfer processes. These reactions may give rise to high-molecular-weight material, which significantly influences L_W. To partially circumvent such problems, the high-molecular-weight part of the MWD may be cut off or may be suitably modified. This procedure obviously introduces some arbitrariness into k_t analysis.

An alternative procedure of estimating k_t from PLP–SEC data has been introduced by Lämmel [23,117]. Based on an adequate kinetic scheme, the entire MWD and the conversion of the PLP experiment were simulated via PREDICI®. The termination rate coefficient, k_t, and the laser induced free-radical concentration, c_R^0, are obtained by fitting measured MWD and experimental conversion. This procedure may be rather time consuming. In addition, problems associated with non-laser-induced polymerization (that give rise to high-molecular-weight polymer) may interfere with this type of analysis. To avoid such difficulties, Lämmel suggested to consider the MWD trace only within the range of the characteristic PLP structure. From the simulations, he recommended fitting the ratio of areas, *RA*, under the number MWD curve, e.g. the area between the second and third point of inflection divided by the area between the first and second point of inflection. k_t and c_R^0 are obtained by fitting the experimental *RA* and conversion data via PREDICI® or by adopting a lumping scheme [23,119]. It should be noted that the application of this procedure requires δ, the contribution of disproportionation to overall termination, and the extent of SEC axial broadening to be (at least approximately) known. The fitting procedure according to the lumping scheme is easily and effectively performed.

As has been shown, for styrene polymerizations at 1000 bar and various temperatures [120], k_t values

deduced from PLP via one of the three independent procedures yields reasonable estimates of termination rate coefficients. It needs to be realized that the k_t determinations from PLP–SEC are restricted to situations of low monomer conversion. While k_p stays constant over extended conversion ranges, k_t is diffusion controlled and has to be measured as a function of monomer conversion. PLP methods which enable k_t analysis up to higher conversion are illustrated in Section 3.

2.5.3. Polymerization in heterogeneous phase

Initiation by laser pulses as carried out in homogeneous systems is difficult in emulsion polymerizations, because the laser light is strongly scattered and efficient radical generation cannot be achieved. Electrons, however, do not experience such kind of limitations and free radicals may be generated periodically, allowing for k_p determination in these systems. Pulsed-electron beams have turned out to be an alternative means of modulating initiation and termination [3,4].

As has been discussed in Section 2.4, PLP–SEC experiments yield the product $k_p c_M$, from which local monomer concentrations may be determined, if k_p is known. This approach has been applied by van Herk and colleagues to measure local monomer concentrations in microemulsions [121] and miniemulsions [122], droplets and latex particles [3,123], and vesicle structures [124].

2.6. Assessment of the rate coefficients from PLP–SEC

2.6.1. Conversion dependence of k_p

PLP–SEC experiments are usually carried out at monomer conversions below 3%. The measured coefficients should be applicable also at higher conversion, as propagation is a chemically controlled process. However, experimental evidence for high-conversion k_p is scarce. ESR experiments for MMA polymerizations proved that k_p is unchanged at least up to 80% conversion [125–127]. Investigations into ethene homopolymerization applying the SP–PLP technique (Section 3) showed a conversion independent k_p up to about 50% monomer conversion [77,78]. SP–PLP investigations into butyl acrylate polymerizations showed a constant k_p over an extended conversion range up to 80% [128]. For other monomers, k_p is expected to stay constant up to high degrees of monomer conversion, too. Especially in solution polymerizations or in polymerizations to low molecular weight material no variation of k_p with conversion should occur.

2.6.2. Chain-length dependence of k_p

Whereas it is now generally accepted that the termination rate coefficient is chain-length dependent (Section 3.7), it is not yet clear whether and to which extent also the propagation rate coefficient may vary with chain length. There seems to be no doubt about the very first propagation steps to be faster than the reactions of longer radicals. Gridnev and Ittel [129] estimated the rate coefficients $k_p(1)$ and $k_p(2)$ which refer to the first and the second propagation step, respectively. For homopolymerizations of MMA and MAN at 60 °C, a strong variation of k_p for the very first propagation steps was observed.

MMA

$$k_p(1) = 14\,000\ \mathrm{l\ mol^{-1}\ s^{-1}}$$

$$k_p(2) = 3600\ \mathrm{l\ mol^{-1}\ s^{-1}}$$

$$k_{p,PLP} = 843\ \mathrm{l\ mol^{-1}\ s^{-1}}$$

MAN

$$k_p(1) = 340\ \mathrm{l\ mol^{-1}\ s^{-1}}$$

$$k_{p,PLP} = 55\ \mathrm{l\ mol^{-1}\ s^{-1}}$$

$k_{p,PLP}$ refers to the k_p value derived from PLP–SEC experiments. For MMA and MAN, $k_p(1)$ is above the literature value for $k_{p,PLP}$ by about one order of magnitude and by a factor of six, respectively. Kinetic data for the addition of small radicals to monomers also indicate that k_p is significantly higher in the very initial period of chain growth [130].

Nitroxide trapping experiments reported by Moad et al. [131] yield addition rates of low-molecular-weight radicals (resembling propagating radicals of chain length 1 and 2) to methyl acrylate at 60 °C. It was observed that $k_p(1)$ is in the range of $1.5–6.3 \times 10^4\ \mathrm{l\ mol^{-1}\ s^{-1}}$ and $k_p(2)$ is approximately $1.4 \times 10^4\ \mathrm{l\ mol^{-1}\ s^{-1}}$. These values are close to $k_{p,PLP} = 3.6 \times 10^4\ \mathrm{l\ mol^{-1}\ s^{-1}}$, which is estimated from PLP–SEC experiments for 60 °C (Table 5). This result shows that the large difference between $k_{p,PLP}$ and $k_p(1)$ or $k_p(2)$ that is seen for MMA and MAN must not occur with all monomers.

Modeling of styrene polymerizations by Deady et al. [12] revealed that the occurrence of very high $k_p(1)$ and $k_p(2)$ values does not affect the MWD significantly in systems, where k_p is relatively high. Only for systems with very low propagation rate coefficients, such as methacrylonitrile, a slight influence of high $k_p(1)$ and $k_p(2)$ on the MWD and thus on the determination of $k_{p,PLP}$ may occur.

Olaj et al. [132] recently addressed the chain-length dependence of k_p. Experimental data presented for MMA and styrene homopolymerizations at 25 °C in bulk and in solution indicate a dependence of k_p on chain length. A variation of k_p by up to 20% is observed. A stronger change of k_p is seen at shorter chain lengths. At large chain lengths a plateau value is reached. With styrene the limiting value at high radical chain-length is approximately $75\ \mathrm{l\ mol^{-1}\ s^{-1}}$ for polymerizations in bulk and in toluene, and is $80\ \mathrm{l\ mol^{-1}\ s^{-1}}$ in cyclohexane, and $65\ \mathrm{l\ mol^{-1}\ s^{-1}}$ in ethyl acetate. The finding of a decrease in k_p with radical chain length is suggested to be related to a progressive shielding of the active center by the polymeric chain. Chain segments already incorporated into the propagating polymer radical displace monomer molecules in the vicinity of the chain end resulting in a lower 'apparent' propagation rate [132]. As has been discussed in Section 2.4.2, k_p estimates via Eq. (1) assign the reduced propagation rate to k_p, since $c_{M,loc}$ (close to the radical chain end) is not precisely known.

2.7. Concluding remarks on k_p

The PLP–SEC technique provides access to reliable k_p data for free-radical homo- and copolymerizations. The resulting propagation rates are very helpful for modeling polymerization processes. The solvent influence on k_p and a potential chain-length dependence of k_p are not yet fully understood. The associated variations in k_p are mostly rather small. The solvent effect on propagation rate in most cases is less than 25%. The currently available experimental data indicate that, with the exception of the very first propagation steps, the variation of k_p over an extended range of radical chain lengths is mostly below 20%.

3. SP–PLP experiments directed toward the determination of termination rate coefficients

After a brief introduction into the method (Section 3.1), k_t data determined over extended ranges of

monomer conversion will be presented in Section 3.2. The remainder of this chapter focuses on the initial plateau region of (almost) constant k_t, which is investigated for homopolymerizations (Section 3.3), and for copolymerizations (Section 3.4). The temperature and pressure dependence of copolymerization k_t is addressed in Section 3.5 and data for termination rate in solution are presented in Section 3.6. The final Section 3.7 deals with the chain-length dependence of k_t.

3.1. Method and experimental set-up

Other than the PLP–SEC procedure, which is carried out at low degrees of monomer conversion, the SP–PLP experiment [8] may be performed during the entire course of a homogeneous free-radical polymerization up to fairly high degrees of monomer conversion. The monomer conversion induced by a SP, typically of about 20 ns width, is vibrational-spectroscopically measured with a time resolution of 10 μs over a time range of milliseconds up to seconds, depending on the polymerization rate of the particular monomer under investigation. Mostly the laser pulse is applied to a monomer–photoinitiator system with the photoinitiator being chosen such that the primary concentration of photoinitiator-derived free radicals, c_R^0, is almost instantaneously produced. In case of suitable molar absorptivity at the UV excimer laser wavelength, the monomer may also be directly excited. In general, it is however advantageous to use a photoinitiator and to carry out the laser irradiation in a spectral region where the monomer is transparent. 2,2-dimethoxy-2-phenylacetophenone (DMPA) and azobisisobutyronitrile (AIBN) have mostly been used as photoinitiators. They are dissociated by excimer laser irradiation at 351 nm (XeF line).

Fig. 9 shows one of the first such SP–PLP traces from the pioneering work of Schweer into the kinetics of ethene high-pressure free-radical polymerization. A 248 nm (KrF) laser has been used to induce polymerization at 230 °C and 2550 bar. Ethene has been directly excited, as no suitable photoinitiator is available for such high temperatures. Plotted as a function of time t, after firing the laser at $t = 0$, is the monomer conversion induced by the laser pulse. Actually, conversion has been monitored by the increase of polymer absorption in the second overtone region of C–H stretching modes around 8250 cm^{-1}. The time resolution of NIR spectroscopic measurement of polymer concentration is close to 6 μs, which is about twice the time interval required for a single ethene addition step to take place at high

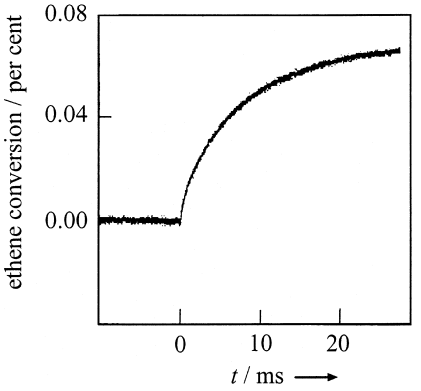

Fig. 9. Monomer conversion vs. time profile measured during an SP–PLP experiment for an ethene polymerization at 190 °C, 2550 bar, and 9.5 wt% polyethylene [77,78].

temperature and pressure. It should be noted that the SP, under perfect initiation conditions, creates a narrow distribution of (living) free radicals with the degree of polymerization linearly increasing with time t unless chain transfer to monomer comes into play. Another important observation from Fig. 9 is that the conversion per pulse is small, but may be measured with a high signal-to-noise quality. The small conversion per pulse allows for a point-wise probing of the kinetics, which is particularly important for k_t that may significantly vary with conversion. The high conversion resolution of the SP–PLP allows to map out the k_t dependence on conversion by a series of successive SP–PLP experiments. For example, the signal in Fig. 9 has been measured during an ethene polymerization after a conversion of 9.5% had already been reached. The signal describes the conversion vs. time behavior of the system after applying the laser pulse at 9.5% conversion and thus represents polymerization kinetics in the range from 9.5 to 9.6% ethene conversions.

With the simplifying assumptions of (a) an instantaneous production of the initial free-radical concentration, c_R^0, of (b) chain-length independent propagation following the well-established rate law (Eq. (18)), and of (c) termination also being chain-length independent and being adequately described by the rate law (Eq. (19)) yields Eq. (20) which represents the time evolution of relative monomer concentration within an SP–PLP experiment

$$\frac{dc_M}{dt} = -k_p c_M t \tag{18}$$

$$\frac{dc_R}{dt} = -2k_t c_R^2 \tag{19}$$

$$\frac{c_M(t)}{c_M^0} = (2k_t c_R^0 t + 1)^{-k_p/2k_t} \tag{20}$$

In the absence of any chain-length dependence of k_t (and of k_p), fitting the experimental conversion vs. time trace to Eq. (20) immediately yields k_p/k_t and $k_t c_R^0$ for the particular experiment. Whereas the assumption that k_p is chain-length independent, generally is a good one, the chain-length dependence of k_t cannot be ignored. As the chain-length varies with time, the rate coefficient which results from fitting of the conversion vs. time trace to Eq. (20) should be referred to as $\langle k_t \rangle$. Within the SP–PLP experiment, the free-radical chain-length increases linearly with time t. As a consequence, termination rate coefficients $k_t(i,i)$ referring to the reaction of two free radicals of more or less identical size may be deduced from analysis of the conversion vs. time trace in different time regions after applying the laser pulse. By adopting a suitable expression for the chain-length dependence of k_t, mostly some power law dependence, an equation similar to Eq. (20), but with chain-length dependent (CLD) k_t, is obtained [78] to which the experimental data may be fitted and the (model-dependent) exponent of a CLD k_t be deduced.

A model-free CLD k_t may be derived from SP–PLP traces of very high signal-to-noise quality, as has been suggested by deKock [10]. Unfortunately, the data quality, which is presently available, does not afford for the associated second derivative analysis. As will be shown in Section 3.7, there are however ways to measure CLD k_t even within extended regions of monomer conversion.

To summarize, the SP–PLP experiment is extremely versatile and powerful. Depending on the signal quality that may be obtained for a given monomer and for given polymerization conditions, the

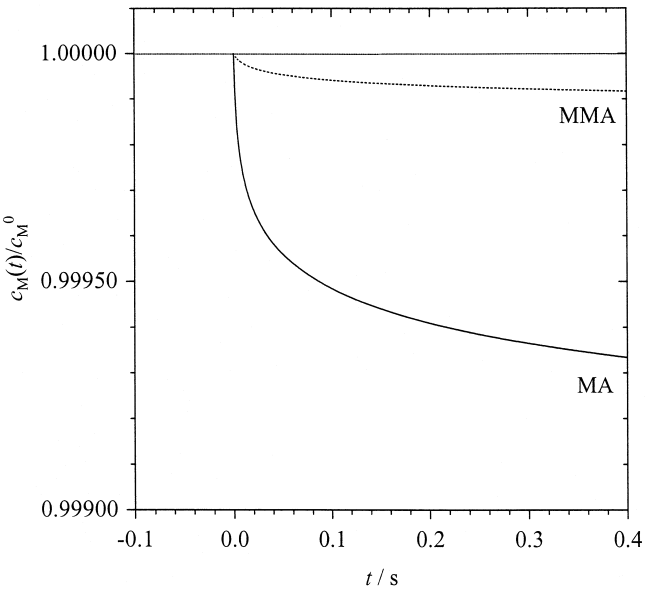

Fig. 10. Time-resolved concentration vs. time profile calculated from Eq. (20) for MMA (dotted line) and MA (full line) SP–PLP experiments at 40 °C, 1000 bar, and 2.5% polymer content. Reproduced with permission from Macromolecules 1998;31:3211. © 1998 American Chemical Society [133].

dependence of a chain-length averaged k_t on monomer conversion may be mapped out and also information about chain-length dependence of k_t may be accessible.

As can be seen from Eq. (20), the degree of monomer conversion per laser pulse depends on k_t, k_p and on primary radical concentration; c_R^0. Low k_t and high k_p are advantageous for obtaining an intense SP–PLP signal. In order to illustrate this influence, two SP–PLP signals were calculated from Eq. (20) and are plotted in Fig. 10 [133]. The signals refer to SP–PLP experiments in the initial period of methyl acrylate and methyl methacrylate homopolymerizations at 40 °C, 1000 bar and a primary free-radical concentration, c_R^0, of 6×10^{-6} mol l^{-1}. The rate coefficients, k_p and k_t, that go into the calculation of the conversion-time profiles are: $k_p(\text{MA}) = 24\,500$ l mol^{-1} s^{-1}, $k_t(\text{MA}) = 1.1 \times 10^8$ l mol^{-1} s^{-1}, $k_p(\text{MMA}) = 902$ l mol^{-1} s^{-1} and $k_t(\text{MMA}) = 2.5 \times 10^7$ l mol^{-1} s^{-1}. Up to 0.4 s, the MA concentration decays by about 0.07%. By adding up a few (up to 10) individual SP–PLP signals, Kurz [134] succeeded to reliably measure such a conversion vs. time curve, although with an increased scattering as compared to the calculated signal in Fig. 10. For dodecyl acrylate, with the rate coefficients under the same conditions being: $k_p = 41\,300$ l mol^{-1} s^{-1} and $k_t = 2.47 \times 10^6$ l mol^{-1} s^{-1}, the monomer conversion induced by one pulse is much larger than with MA and exceeds 2%. The intense SP–PLP signal observed with DA allows for the determination of k_t/k_p from a 'true' (i.e. not averaged) single pulse trace. The opposite holds for MMA (Fig. 10), where the monomer conversion induced per pulse is below 0.01% after 0.4 s. By co-adding a larger number (about 100) of individual SP–PLP signals, however, even for such an unfavorable kinetic situation, useful 'single pulse' signals may be obtained [133].

Plotted in the upper part of Fig. 11 is the change in relative monomer concentration, $c_M(t)/c_M^0$, measured as a function of time t for an MMA bulk polymerization at 40 °C and 1000 bar. The signal results from co-adding 80 individual SP–PLP traces recorded within a total of 400 s. The kinetic

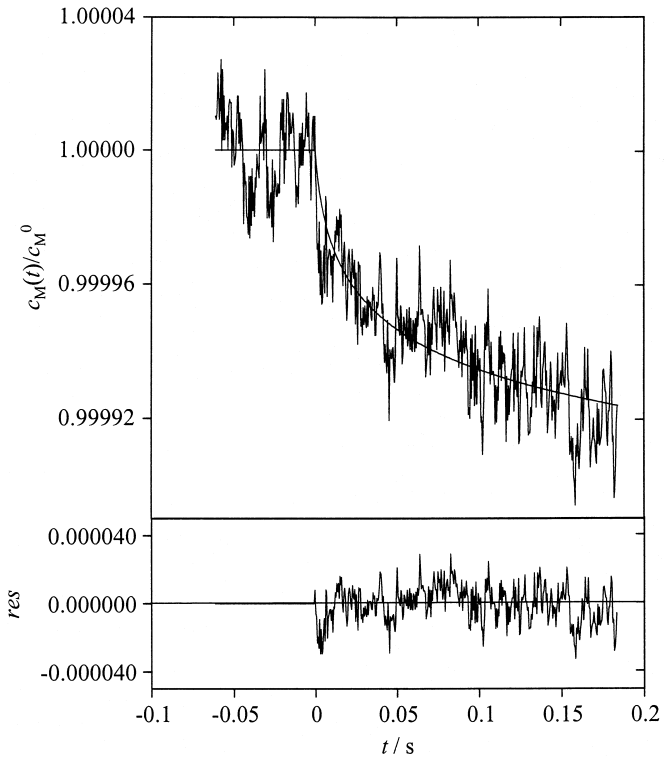

Fig. 11. Monomer concentration vs. time trace measured during a methyl methacrylate polymerization at 40 °C and 1000 bar at MMA conversions between 7.7 and 9.7%. The signal is obtained by co-adding 80 single pulse traces. The difference between measured and fitted (Eq. (20)) data is illustrated by plotting the residuals (*res*) in the lower part of Fig. 11. Reproduced with permission from Macromolecules 1998;31:3211. © 1998 American Chemical Society [133].

information in Fig. 11 refers to overall MMA conversions between 7.7 and 9.7%. MMA concentration is determined with a time resolution of 60 μs via the NIR monomer absorption around 6170 cm^{-1}. The curve fitted to the data in Fig. 11 is obtained via Eq. (20). The quality of this fit is illustrated by the plot of residuals in the lower part of Fig. 11. No systematic deviation between measured and fitted data can be detected. The fit directly yields k_t/k_p, from which, in conjunction with k_p from PLP–SEC, k_t is obtained. The resulting MMA termination rate coefficients are assumed to be accurate within ±40%. As is described in more detail in Ref. [133], it is within these limits of uncertainty that the data from SP–PLP agree with the best available literature values deduced by other techniques. The situation illustrated in Fig. 11 is close to a worst-case scenario. Interestingly, the signal quality improves at higher degrees of monomer conversion because of the significant drop in k_t associated with the onset of the gel effect (Section 3.2). Feldermann succeeded to measure SP–PLP traces of good signal-to-noise quality during MMA bulk polymerization at conversions above 30% [135].

Similar problems as with MMA are met in SP–PLP experiments on styrene. In situations where the conversion induced by a SP is extremely small, a different type of pulsed laser experiment, the pulse sequence (PS)–PLP technique, may be used [128,136–138]. The pseudo-stationary method which has been detailed in Ref. [137] works as follows: the change in monomer concentration resulting from the

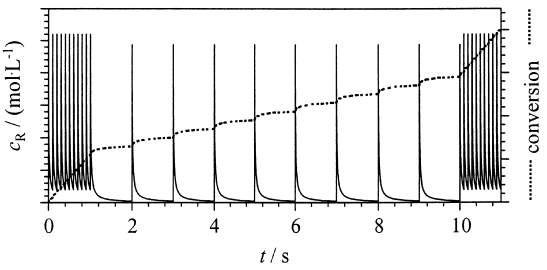

Fig. 12. Free-radical concentration vs. time t profile during a PS–PLP experiment, where a sequence of nine pulses at low pulse repetition rate is embedded in between two sequences of high laser pulse repetition rate. Reproduced with permission from ACS Symposium Series 685, 1998. p. 84. © 1998 American Chemical Society [120].

application of a known and large (usually between 100 and 1000) number of evenly spaced laser pulses is spectroscopically measured by taking NIR spectra before and after irradiation of such a pulse sequence. From this concentration difference, the conversion per pulse, Δc_M, reached within the time interval determined by the inverse of the selected pulse repetition rate, ν, is accurately determined.

As is thoroughly discussed in Ref. [137], with k_p and with the primary laser-induced free-radical concentration (and thus initiation efficiency) being known from independent experiments, k_t may be directly obtained from Δc_M measured at a given pulse repetition rate, ν. Mostly this additional information is not at hand. The preferred mode of carrying out the PS–PLP experiment under such conditions thus is to apply pulse sequences of alternating pulse repetition rates, ν_{high} and ν_{low}. This *alternating* PS–PLP method yields k_p/k_t as does the SP–PLP technique without, however, providing the other benefits of the latter technique such as the measurement of time-resolved macromolecular growth with the potential of studying chain-length dependent k_t. The PS–PLP technique, however, has advantages over the other pseudo-stationary method, the traditional rotating-sector method, in that it is considerably less labor intensive and, more importantly, in that it may be applied to measure the conversion dependence of k_t up to higher degrees of monomer conversion. Advantages with respect to the SP–PLP technique are that PS–PLP is not associated with microsecond time-resolved measurement of monomer concentration and that PS–PLP functions better for monomers of very low k_p/k_t. With the improvement of signal-to-noise quality of the SP–PLP procedure, the importance of the PS–PLP method will, however, decay. Experimental details about the PS–PLP procedure can be found in Refs. [137,138].

The free-radical concentration vs. time t profile during a PS–PLP experiment is schematically given in Fig. 12. A sequence of nine pulses applied at low pulse repetition rate is embedded in between two sequences of high laser pulse repetition rate. As a dotted line, the time dependence of monomer conversion is given. Spectroscopic measurements of monomer content are carried out before and after applying a sequence of pulses.

A brief account of the experimental set-up used in SP–PLP studies (Fig. 13) will now be given. The principal components are an excimer laser of about 20 ns pulse width (mostly operated on the XeF-line at 351 nm), a tungsten halogen lamp (La, 75 W, general electric) powered by two batteries (12 V, 180 A/h), a BM 50 monochromator (B&M Spectronic) and a detector unit equipped with a fast InAs-detector (Det) (EG & G, Judson) with a time resolution up to 2 μs. By means of UV mirrors (M), which are transparent in the IR/NIR region, the laser pulses are directed through the high-pressure polymerization cell (HC). A UV detector (D) positioned in front of the cell serves for measuring the intensity of

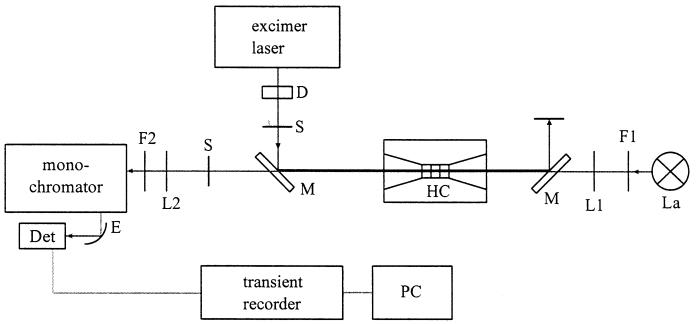

Fig. 13. Experimental set-up for single pulse (SP)–pulsed-laser polymerization (PLP). For details see text.

each individual laser pulse. By means of a photo-shutter (S), individual pulses or a pre-selected number of pulses may be applied. The IR/NIR probing light, by means of a CaF_2 lens (L1, $f = 100$ mm, $d = 50$ mm) is focused into the cylindrical optical high-pressure cell equipped with two sapphire windows. A second CaF_2 lens (L1) of identical dimensions focuses the IR/NIR light after penetration through the cell onto the lid of the monochromator where it is diffracted at an interference grating (Bausch&Lomb, 76 mm × 76 mm, 600 mm^{-1}, blaze 1.6 mm, $D = 4.1$ nm mm^{-1}). By means of an ellipsoidal mirror (E), the NIR light is transmitted onto the fast NIR detector. A silicium filter F2 (Oriel, 1 mm, 1.05 μm, transmission in the 5000–9000 cm^{-1} region) ensures that only one grating order hits the detector. The detector signal is digitized on a 12-bit transient recorder (ADAM TC 210-1, René Maurer AG) and transferred to a PC for further data processing.

The irreversible change in intensity of the NIR probing light associated with polymerization induced by each preceding laser pulse is electronically compensated for the subsequent pulse. Prior to polymerization, the monomers are distilled under reduced pressure in the presence of dry K_2CO_3 to remove the inhibitor and are treated by several freeze-and-thaw cycles to remove dissolved oxygen. The photoinitiator, mostly DMPA, is added to yield initial DMPA concentrations typically of 5×10^{-3} mol l^{-1}. The DMPA concentration may, however, be by about one order of magnitude below or above this value (Section 3.7). The polymerizing mixture is mostly contained in an internal cell that is inserted into the high-pressure optical cell [139]. UV-irradiation with the excimer laser is usually carried out at single pulse energies of 2–3 mJ being incident on the sample. Monomer conversion is monitored with a time-resolution of a few microseconds mostly at NIR wavenumbers characteristic of the monomer, around 6170 cm^{-1}. After measuring several conversion vs. time traces, the optical cell is introduced into the sample chamber of an IFS 88 Fourier transform IR/NIR spectrometer (Bruker) where the absolute monomer concentration is checked by analysis in an extended NIR region, typically between 6100 and 6250 cm^{-1}. During each SP–PLP experiment, conversion vs. time traces are recorded until the polymerizing system becomes inhomogeneous or the photoinitiator is consumed. More details about the SP–PLP set-up, in particular about the electronic part, are contained in Kowollik's PhD Thesis [140].

3.2. Termination rate studied over extended ranges of monomer conversion

By subsequent SP–PLP experiments being carried out during a free-radical polymerization, k_t/k_p and thus k_t may be mapped out for an extended region of monomer conversion. A single SP–PLP trace measured during an ethene polymerization at 9.5% conversion (or polyethylene content) has already

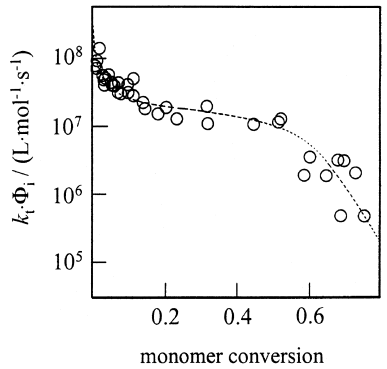

Fig. 14. Rate parameter $k_t\Phi_i$ as a function of monomer conversion measured via SP–PLP during ethene homopolymerizations at 230 °C and 2550 bar [77,78].

been shown in Fig. 9. The k_t values resulting from a series of such individual experiments performed during an ethene homopolymerization at 230 °C and 2550 bar are shown in Fig. 14. Actually the product of $k_t\Phi_i$ is plotted, with Φ_i being the efficiency of photochemical free-radical production. Φ_i is close to unity.

The data which is from several independent ethene SP–PLP studies at 230 °C and 2550 bar reveals an enormous change, by almost three orders of magnitude, in termination rate coefficient over the experimental range up to about 75% ethene conversion. In view of this enormous effect, the conversion dependence of k_t will first be studied without taking any chain-length dependence of rate coefficients into account. The k_t values presented in Sections 3.2–3.6 should be referred to as chain-length averaged termination rate coefficients. The (moderate) influence of free-radical chain length will be addressed in Section 3.7.

k_t of ethene free-radical polymerization decreases within the entire conversion range depicted in Fig. 14. In the initial polymerization period the decrease is pronounced, thereafter is rather weak, before another clear decrease occurs at conversions above 50%. Significant changes of k_t with the degree of monomer conversion have already been reported for MMA free-radical polymerization. Fig. 15 shows the data of Sack-Kouloumbris and Meyerhoff for ambient pressure and 0 °C [141]. Such dependence has also been found by Feldermann from SP–PLP experiments with his data, however, being restricted to conversions below 50% [135]. Contrary to what is seen for ethene, with MMA a plateau region occurs at low conversion. Above 35% MMA conversion, the shape of the k_t vs. monomer conversion curve is very close to the variation seen from the very beginning of ethene polymerization (Fig. 14). This similarity suggests that common termination mechanisms are operative for both compounds. Data from PS–PLP experiments into styrene bulk polymerization at 50 °C and 2800 bar [138] are given in Fig. 16. With respect to the type of k_t vs. monomer conversion dependence, this data also fits into the picture provided by the ethene and MMA data in Figs. 14 and 15, respectively, with the initial plateau region being larger than with MMA.

The initial plateau region may become even more extended. Particularly large ranges of constant, conversion-independent k_t are found in the bulk polymerization of (meth)acrylic esters where the ester group is large, such as dodecyl acrylate (DA) and dodecyl methacrylate DMA. As is shown for the acrylate family in Fig. 17, within the series MA, BA, and DA, the absolute value of k_t in the initial

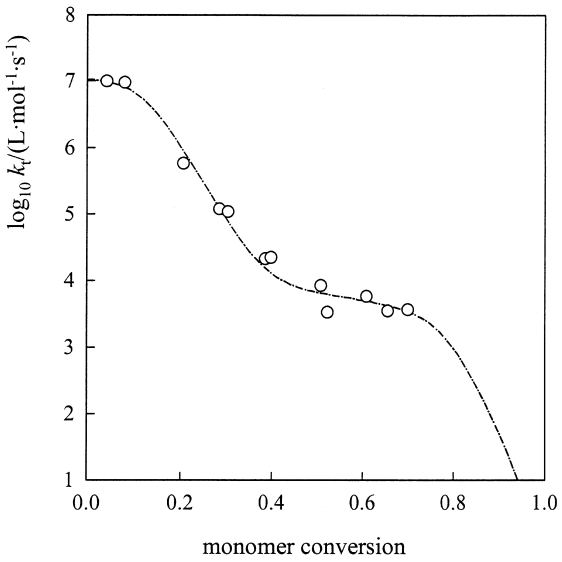

Fig. 15. Conversion dependence of the termination rate coefficient k_t for polymerizations of methyl methacrylate at ambient pressure and 0 °C. Experimental data are from Ref. [142]. The line is fitted according to Eq. (21).

plateau region decreases whereas the extension this region of (almost) constant k_t increases toward higher monomer conversion. With BA, the plateau region is not perfectly flat as, e.g. with BMA (Section 3.3). The reason for this is not yet clear, but may be specific for BA. The data in Fig. 17 is from different sources: MA [142], BA [143], and DA [142] but always refers to 40 °C and 1000 bar.

The transitions from plateau-type behavior to regions where k_t clearly and sometimes enormously

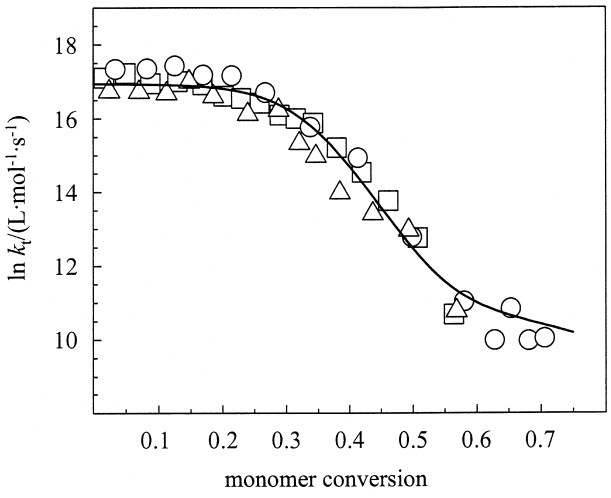

Fig. 16. Variation of the termination rate coefficient, k_t, with monomer conversion in laser-induced bulk polymerizations of styrene at 50 °C and 2800 bar. Data from three independent experiments are shown. The line represents the best fit according to Eq. (21). Reproduced with permission from Macromol Chem Phys 1997;198:1455. © 1997 Wiley–VCH [138].

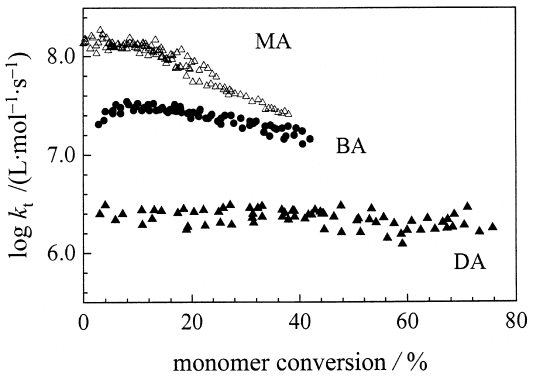

Fig. 17. Variation of k_t with monomer conversion for bulk polymerizations of MA, BA, and DA at 40 °C and 1000 bar [142,143]. Reproduced with permission from Chemical synthesis using supercritical fluids, 1999, p. 326. © 1999 Wiley–VCH [185].

drops upon further increasing monomer conversion, indicate transitions in the type of diffusion control of the termination process. As has been discussed in detail in Ref. [144], the initial plateau region is assigned to segmental diffusion, followed by translational diffusion. The subsequent weaker decrease in k_t is assigned to control by reaction diffusion where termination occurs via propagation. At the highest conversions also propagation may run under diffusion control, which leads to a significant lowering of reaction-diffusion controlled k_t. All four mechanisms are seen with MMA, whereas for the other monomers only part of these mechanisms plays a role. Nevertheless, a common systematic of the conversion dependence of k_t can be given [144]. The observed conversion dependence of k_t on conversion, X, may be reasonably fitted by Eq. (21)

$$k_t = \frac{1}{k_{TD}^{-1} + \eta_r/k_{TD}^0} + \frac{C_{RD}(1-X)}{k_{p,0}^{-1} + \eta_r/k_{p,D}^0} \tag{21}$$

k_{SD}, k_{RD}^0, and $k_{p,0}$ denote the rate coefficients of segmental diffusion, translational diffusion at zero conversion, and propagation at low conversion, respectively. $\eta_r = \eta/\eta_0$ is the relative bulk viscosity with η_0 being the pure monomer viscosity at polymerization temperature T and pressure p. $k_{p,D}^0$ is the (hypothetical) rate coefficient of diffusion-controlled propagation at zero conversion which is defined by the following general expression for diffusion controlled k_p:

$$k_p = (k_{p,0}^{-1} + \eta_r/k_{p,D}^0)^{-1} \tag{22}$$

Finally, C_{RD} in Eq. (23) is an empirical constant which relates the reaction-diffusion controlled termination rate coefficient, $k_{t,RD}$, to k_p and to the fraction of unreacted monomer, $1 - X$:

$$k_{t,RD} = C_{RD} k_p (1 - X) \tag{23}$$

The first term on the RHS of Eq. (21) represents the joint contribution of translational (center-of-mass) and of segmental diffusion to overall termination. Under conditions where segmental mobility controls termination, which may be the case in the initial polymerization period where translational diffusion of macroradicals is fast, k_t is more or less constant and close to k_{SD}. Toward higher conversion, the

translation-diffusion (center-of-mass) contribution to the first term on the RHS of Eq. (21), $k_{TD} = k_{TD}^0/\eta_r$ becomes dominant due to the enormous increase in bulk viscosity (η_r) with monomer conversion.

The second term on the RHS of Eq. (21) denotes the contribution of reaction diffusion to overall k_t. This term differs from the corresponding one in Eq. (23) in that the general, conversion-dependent expression for k_p (Eq. (22)) is used. Under conditions where center-of-mass diffusion is largely hindered, e.g. at high conversion, and with monomers of high k_p, Eq. (23) may account for most of overall k_t. For butyl acrylate bulk polymerization at moderate and high conversion, $k_{t,RD}/(k_p(1 - X))$, which is directly obtained from $k_t \cong k_{t,RD}$, measured at different degrees of monomer conversion, and from k_p, yields a conversion-independent value which is identified with C_{RD} (Eq. (23)) [120,128].

Eq. (21) is capable of representing the different types of experimental k_t vs. monomer conversion behavior. The lines in Figs. 14–16 have been obtained by fitting measured k_t data to Eq. (21). This equation has also been used to represent k_t of ethene over an extended pressure, temperature, and conversion region as is covered in technical high-pressure polymerization [77,78]. The remarkable feature of the ethene SP–PLP experiments is that both parameters from fitting the conversion vs. time traces to Eq. (20) are used for deriving kinetic parameters. According to the strategy outlined in Refs. [77,78], and by adopting the quantum efficiency, Φ_i, of free-radical formation after UV excitation of pure ethene to be close to unity, both individual coefficients, k_t and k_p, are obtained from a single SP–PLP experiment.

The rate expressions for $k_t(T, p, X, \eta_r)$ and for $k_p(T, p, X)$ of ethene are presented as Eqs. (24) and (25), respectively, where the zero conversion values of both rate coefficients, k_t^0 and k_p^0 are given by Eqs. (26) and (27), respectively

$$k_t(T,p,X,\eta) = \left(0.832\frac{1}{\eta_r} + 8.04\times10^{-6}(1-X)\frac{k_p^0}{1+\dfrac{k_p^0}{1.13\times10^{10}}\eta_r} \right) k_t^0 \tag{24}$$

$$k_p(T,p,\eta) = \frac{k_p^0}{1+\dfrac{k_p^0}{1.13\times10^{10}}\eta_r} \tag{25}$$

$$k_t^0\ (\mathrm{l\,mol^{-1}\,s^{-1}}) = 8.11\times10^8 \exp\left(\frac{-553 - 0.190p\ (\mathrm{bar})}{T\ (\mathrm{K})}\right) \tag{26}$$

$$k_p^0\ (\mathrm{l\,mol^{-1}\,s^{-1}}) = 1.88\times10^7 \exp\left(\frac{-4126 + 0.33p\ (\mathrm{bar})}{T\ (\mathrm{K})}\right) \tag{27}$$

The procedure of estimating η_r is described in Ref. [78]. The variation with monomer conversion of k_t and of k_p for 230 °C, 2550 bar is plotted in Fig. 18.

Eqs. (24)–(27) turned out to adequately represent the kinetics of ethene free-radical homopolymerization in rather extended ranges of T, p, and X [145].

Although the model underlying Eq. (21) appears to properly describe the major effects associated with the conversion dependence of k_t, it is definitely a crude model as, e.g. the chain-length dependence of k_t is not considered. Moreover, the molecular weight (distribution) of the polymer (from preceding

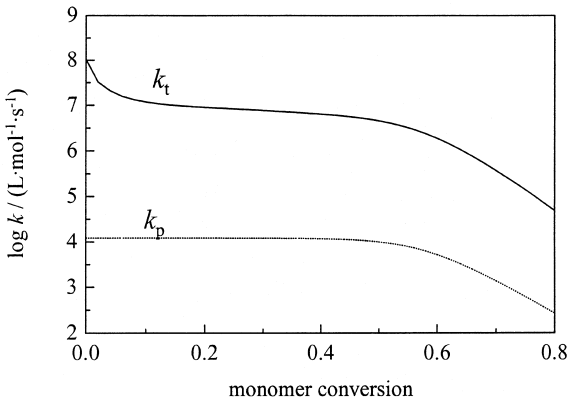

Fig. 18. Variation of the termination and propagation rate coefficients, k_t and k_p, respectively, with monomer conversion for ethene polymerizations at 230 °C and 2500 bar [77,78]. The lines represent best fits of Eqs. (24) and (25) to the experimental data obtained from SP–PLP.

polymerization), which strongly affects the viscosity of the reaction medium, is not explicitly taken into account but is implicit in η_r, the relative viscosity, which is difficult to measure during the course of polymerization reactions, in particular at elevated temperatures and pressures.

That macroradical chain-length affects k_t, may be easily demonstrated via PS–PLP experiments. Shown in Fig. 19 is the conversion dependence of bulk MMA free-radical polymerization at 30 °C, 1000 bar studied by PS–PLP experiments carried out at two significantly different pulse repetition rates, $\nu = 0.21\ s^{-1}$ and $\nu = 13.5\ s^{-1}$ [146]. In the initial plateau region, k_t is almost the same for the two experiments with a weak indication of k_t being slightly higher at $\nu = 13.5\ s^{-1}$ where chain length is significantly smaller than in the $\nu = 0.21\ s^{-1}$ experiment. (The difference in chain length may be easily demonstrated by an accompanying PLP–SEC measurement). The plateau region is less extended at the lower pulse repetition rate ($0.21\ s^{-1}$), as the higher molecular weight species produced under these conditions get entangled at lower conversion and earlier enter into the gel effect region were center-of-mass diffusion controls k_t. In the region were k_t steeply decreases upon increasing conversion, enormous differences in k_t (at identical conversion) are seen. They are due to both differences in chain-length dependence and to differences in bulk viscosity that are associated with the quite different sizes of the polymeric material produced at the two repetition rates. The data in Fig. 19 clearly illustrates the 'history dependence' of k_t. The dynamics of the preceding polymerization (which is contained in the MWD and in other properties of the polymer) influences the subsequent reaction and, in particular, affects diffusion-controlled k_t.

A similar picture as shown for MMA polymerization (Fig. 19) has been obtained for styrene free-radical polymerization. Fig. 20 shows the variation of k_t for styrene at 50 °C, 2000 bar deduced from PS–PLP studies at repetition rates of $\nu = 0.9$ and $13\ s^{-1}$ [138]. Again, the dependence of k_t in the plateau region is very small with, however, a clearer (than with MMA) indication of k_t being enhanced toward larger pulse repetition rate, that is toward smaller free-radical chain length. This effect will be addressed more closely in Section 3.7. In the gel effect region, at monomer conversions above 20%, the impact of (free-radical and polymer) chain length on k_t is clearly seen, although it is less pronounced than with MMA. (It should be noted that k_t is given on a $\log_e$ scale in Fig. 20, whereas in most other figures a $\log_{10}$ scale is used for k_t.)

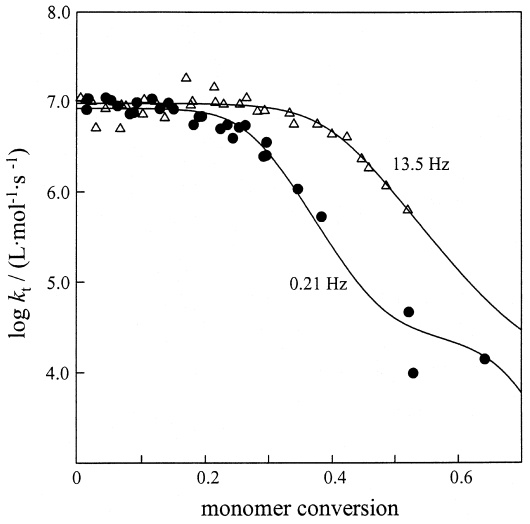

Fig. 19. Variation of termination rate coefficient k_t with monomer conversion in laser-induced MMA bulk polymerizations at 30 °C, 1000 bar carried out at laser pulse repetition rates ν of 0.21 and 13.5 Hz; ν stays constant within each experiment [146]. The lines are fitted according to Eq. (21). Reproduced with permission from Macromol Symp 1996;111:229. © 1996 Wiley–VCH [79].

Figs. 19 and 20 demonstrate that the chain-length dependence is different in regions, which differ in the mechanism of diffusion control of k_t. Within the reaction-diffusion region a third type of chain-length dependence of k_t may be found. This region has however not been carefully explored so far. It may, however, be assumed that, as k_p is not (markedly) dependent on chain length, $k_{t,RD}$ should also be

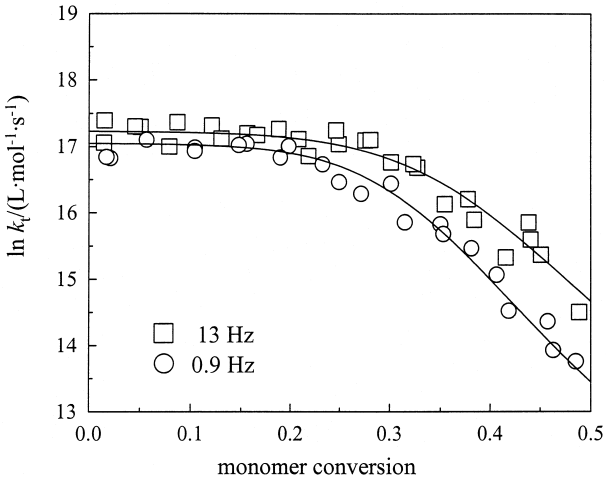

Fig. 20. Variation of termination rate coefficient k_t with monomer conversion in laser-induced styrene bulk polymerizations at 50 °C, 2000 bar carried out at different laser pulse repetition rates, $\nu = 0.9$ and 13 Hz; ν stays constant within each experiment [138]. The lines are fitted according to Eq. (21). Reproduced with permission from Macromol Chem Phys 1997;198:1455. © 1997 Wiley–VCH.

insensitive toward chain length. On the other hand, the constant in the reaction-diffusion term, C_{RD}, may vary with free-radical size. The termination kinetics may become rather complex toward elevated and high conversion, where free-radical chain length and the dynamic properties of the reaction medium, with particular impact coming from polymer microstructure, play an important role. As SP–PLP experiments under such conditions have not yet been carried out, the remainder of this section will be restricted to studies into k_t within the initial polymerization region. With the exception of ethene and of butyl acrylate polymerization, more or less extended plateau k_t regions are found in the early polymerization period. In Section 3.3, homo-termination rate coefficients of styrene and of (meth)acrylates will be presented. Section 3.4 deals with copolymerization k_t, mostly of (meth)acrylate systems.

3.3. Homo-termination rate coefficients at low and moderate degrees of monomer conversion

With a very few exceptions, the pulsed laser induced studies into termination kinetics have been carried out at elevated pressures, which brings a twofold advantage: k_p is significantly enhanced with pressure and k_t is lowered. Thus, k_p/k_t strongly increases toward higher p, which is associated with a largely improved signal-to-noise quality of the SP–PLP conversion vs. time traces. In most cases, both the temperature dependence and the pressure dependence have been determined which allows estimates of k_t to be carried out for other temperatures and also for ambient pressure. All k_t data of this section refers to chain-length averaged termination rate coefficients.

3.3.1. Styrene

The termination rate coefficient of bulk styrene polymerization has been studied extensively via the PS–PLP method [33]. Recently, also SP–PLP experiments were successfully carried out [147], the results of which are in excellent agreement with the PS–PLP data. The temperature dependence of the plateau k_t which refers to the first 20% of bulk styrene polymerization is plotted for various pressures in Fig. 21. Together with the data from PS–PLP (open symbols), several k_t values from chemically initiated polymerization (via thermal decomposition of 2,2′-azoisobutyronitrile) are presented (full symbols) in Fig. 21. The data sets obtained by chemical and by photochemical initiation closely fit to each other. The set of chain-length-averaged plateau k_t values is adequately represented by Eq. (28), which holds for conversions up to 20%, for temperatures between 30 and 90 °C, and pressures up to 2800 bar. The formula should, however, also be applicable to estimates of k_t at temperatures and pressures slightly beyond the T and p ranges of the underlying experiments. It should be mentioned that a slight curvature on the ln k_t vs. p correlations for constant temperature is seen [138], which corresponds to a weakly pressure-dependent activation volume. In Eq. (28), this effect is accounted for by the quadratic term in p

$$\ln k_t\,(\mathrm{l\,mol^{-1}\,s^{-1}}) = 20.785 - 1.050\times10^{-3}p\,(\mathrm{bar}) + 5.2\times10^{-8}p^2\,(\mathrm{bar^2}) - \frac{753}{T\,(\mathrm{K})} + \frac{0.1060}{T\,(\mathrm{K})}p\,(\mathrm{bar}) \tag{28}$$

For 30 °C, from the pressure dependence of k_t (Eq. (3)), an activation volume of $\Delta V^{\#}(k_t) = (14 \pm 2.6)\ \mathrm{cm^3\ mol^{-1}}$ is derived. The activation energy of k_t at ambient pressure is obtained to be: $E_A(k_t) = (8.9 \pm 3.2)\ \mathrm{kJ\ mol^{-1}}$. Interestingly, both activation parameters are very close to activation parameters calculated from the pressure and temperature dependence of the inverse of pure styrene

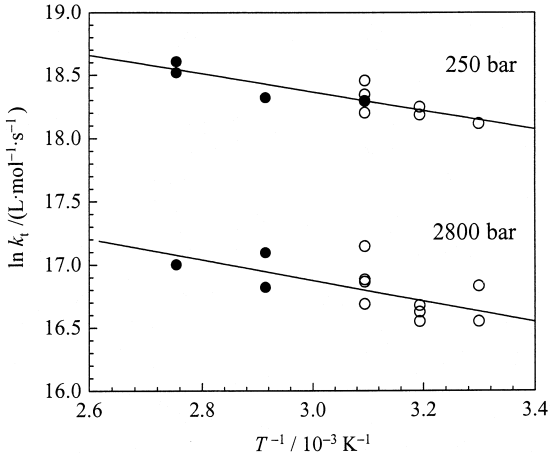

Fig. 21. Temperature dependence of low conversion k_t data for styrene bulk polymerizations at 250 and 2800 bar (as indicated); open marker refer to k_t determined via PS–PLP experiments and filled marker to k_t derived from chemically initiated polymerizations [138]. Data refer to the initial plateau region of constant k_t (for details see text). Reproduced with permission from Macromol Chem Phys 1997;198:1455. © 1997 Wiley–VCH.

viscosity: $\Delta V^{\#}(\eta_{STY}^{-1}) = 14.6\ \text{cm}^3\ \text{mol}^{-1}$ and $E_A(\eta_{STY}^{-1}) = 9.9\ \text{kJ mol}^{-1}$, respectively. This agreement is fully consistent with the view that segmental diffusion constitutes the rate determining step and that for a given type of segments, e.g. the ones in polystyrene or in associated macroradicals, the temperature and pressure dependence of k_t is given by the (inverse of) monomer viscosity which essentially controls segmental mobility inside the coil. It is important to note that it is not the bulk viscosity of the polymerizing medium which affects termination kinetics.

3.3.2. Alkyl acrylates

The termination kinetics of methyl acrylate and dodecyl acrylate has been extensively studied by Kurz [134] and additional k_t data for these monomers have been provided by Kowollik [140] and by Külpmann [148]. Temperature and pressure dependent (chain-length-averaged) plateau k_t values for both substances are presented in Ref. [149]. Illustrated in Fig. 22 is the temperature dependence of k_t measured for both monomers at 1000 bar. The activation energies referring to 1000 bar are: (9 ± 6) kJ mol^{-1} for MA and (4 ± 5) kJ mol^{-1} for DA with these values not being significantly different within the rather extended limits of experimental accuracy

$$\log k_t\ (\text{l mol}^{-1}\ \text{s}^{-1}) = 9.48 - 454(T^{-1}\ (\text{K}^{-1}))$$
$$(\text{MA bulk polymerization at 1000 bar},\ 10\ ^\circ\text{C} \le \theta \le 50\ ^\circ\text{C}) \tag{29}$$

$$\log k_t\ (\text{l mol}^{-1}\ \text{s}^{-1}) = 7.03 - 199(T^{-1}\ (\text{K}^{-1}))$$
$$(\text{DA bulk polymerization at 1000 bar},\ 15\ ^\circ\text{C} \le \theta \le 50\ ^\circ\text{C}) \tag{30}$$

The pressure dependence of k_t, which has been measured for both monomers at 40 °C, is shown in

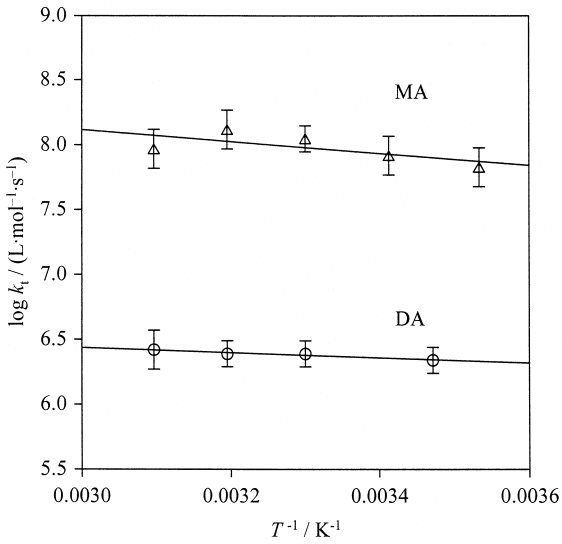

Fig. 22. Temperature dependence of k_t for homopolymerizations of MA and DA at 1000 bar derived from SP–PLP experiments in the initial plateau region of constant k_t (for details see text).

Fig. 23. The associated fitted lines are given as Eqs. (31) and (32) for MA and DA, respectively. It cannot be excluded that also the variation of k_t with p is slightly curved. It is in particular the DA data, which provides some indications of such an effect. As the curvature is, however, not safely backed by the experimental data (Fig. 23), pressure-independent activation volumes have been deduced from linear fits of the log k_t vs. p data. The resulting rate expressions for MA and DA are given as Eqs. (31)

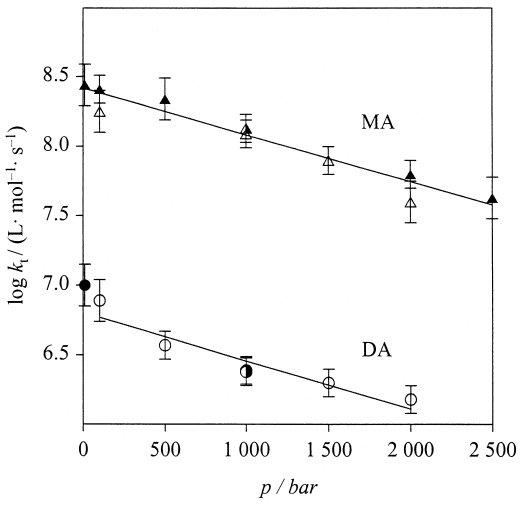

Fig. 23. Pressure dependence of k_t for homopolymerizations of MA and DA at 40 °C derived from SP–PLP experiments in the initial plateau region of constant k_t (for details see text); full symbols are from Ref. [148], open symbols from Ref. [134], and half filled symbols from Ref. [140].

and (32), respectively

$$\log k_t \text{ (l mol}^{-1}\text{ s}^{-1}) = 8.42 - 3.34 \times 10^{-4}(p \text{ (bar)}) \quad \text{(MA bulk polymerization at 40 °C, 100 bar} \leq p \leq \text{2500 bar)} \tag{31}$$

$$\log k_t \text{ (l mol}^{-1}\text{ s}^{-1}) = 6.82 - 3.48 \times 10^{-4}(p \text{ (bar)}) \quad \text{(DA bulk polymerization at 40 °C, 100 bar} \leq p \leq \text{2000 bar)} \tag{32}$$

Eqs. (31) and (32) are associated with activation volumes of (20 ± 6) and (21 ± 6) $cm^3\ mol^{-1}$, respectively.

Butyl acrylate (BA) differs in k_t behavior from the other alkyl (meth)acrylates in that no perfect plateau is seen in the initial polymerization period up to about 10% conversion. This has been illustrated in Fig. 17 by k_t data from SP–PLP measured at 40 °C, 1000 bar [143]. At monomer conversions between 10 and 20%, however, a plateau-type k_t value seems to occur. Such plateau values have been determined from SP–PLP for BA bulk polymerizations in an extended range of pressures and temperatures. The resulting temperature dependence of k_t (at 1000 bar) and the pressure dependence (at 40 °C) are given in Eqs. (33) and (34), respectively

$$\log k_t \text{ (l mol}^{-1}\text{ s}^{-1}) = (8.41 \pm 0.477) - (292 \pm 144)T^{-1}\ (\text{K}^{-1}) \quad \text{(BA bulk polymerization, 1000 bar, 10 °C} \leq \Theta \leq \text{60 °C)} \tag{33}$$

$$\log k_t \text{ (l mol}^{-1}\text{ s}^{-1}) = (7.74 \pm 0.0066) - (2.66 \pm 0.487) \times 10^{-4} p \text{ (bar)} \quad \text{(BA bulk polymerization, 40 °C; 200 bar} \leq p \leq \text{2000 bar)} \tag{34}$$

Eqs. (33) and (34) are associated with an activation energy of (6 ± 3) kJ mol^{-1} and an activation volume of (16 ± 3) $cm^3\ mol^{-1}$, respectively. The difference of BA k_t vs. monomer conversion behavior as compared to the dependencies seen with MA, DA, and also with the alkyl methacrylates, is not yet fully understood. That specific effects are operative with BA is indicated by the k_t data measured for BA in solution of $scCO_2$ which show an appreciable increase with conversion in the initial conversion region [143].

3.3.3. Alkyl methacrylates

Because of the problems with SP–PLP signal quality in methacrylate k_t studies, only relatively few pulsed-laser-assisted measurements have been carried out so far. An Arrhenius plot of k_t for MMA at 1000 bar [133] is shown in Fig. 24.

The fitted line is represented by Eq. (35):

$$\log k_t \text{ (l mol}^{-1}\text{ s}^{-1}) = 8.33 - 291T^{-1}\ (\text{K}^{-1}) \tag{35}$$

The activation energy (at 1000 bar) associated with Eq. (35) is $E_A(k_t) = (5.6 \pm 2.6)$ kJ mol^{-1}. Only two SP–PLP data points, for 1000 and 1500 bar, are available for deriving an activation volume. The resulting (approximate) value is: $\Delta V^{\#}(k_t) = (15 \pm 5)$ $cm^3\ mol^{-1}$. It should be noted that both activation

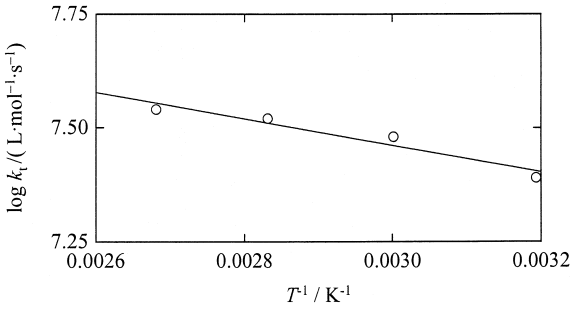

Fig. 24. Temperature dependence of k_t for homopolymerizations of MMA at 1000 bar. Each data point is obtained as a mean value over an initial polymerization range extending up to about 20% monomer conversion. Reproduced with permission from Macromolecules 1998;31:3211. © 1998 American Chemical Society [133].

parameters are close to the corresponding data derived from PS–PLP investigations into styrene bulk polymerization.

For BMA and DMA even less k_t data from PLP is available. In Ref. [150], the numbers for k_t at 40 °C, 1000 bar are given: $\log k_t$ (l mol^{-1} s^{-1}) = 6.70 (bulk BMA, [151]) and $\log k_t$ (l mol^{-1} s^{-1}) = 6.22 (bulk DMA, [140]). From this reference data at 40 °C, 1000 bar, bulk k_t values for other pressures may be estimated via the following activation volumes: $\Delta V^{\#}(k_t) = 18$ cm^3 mol^{-1} for BMA [23] and $\Delta V^{\#}(k_t) = 10.8$ cm^3 mol^{-1} for DMA at 30 °C [140].

Obviously more data is required in order to allow for quantitative plateau k_t data within extended regions of temperature and pressure. That this plateau region may extend up to 30 and to 45% monomer conversion in bulk free-radical polymerizations of BMA and DMA, respectively, has been demonstrated by Bergert [152].

3.4. Termination rate coefficients in binary and ternary (meth)acrylate copolymerizations at low and moderate degrees of monomer conversion

The initial plateau region of constant k_t may be fairly extended, up to at least 40% monomer conversion in DA and DMA bulk homopolymerizations, but is rather small, up to approximately 15% conversion, in MMA bulk polymerization. The extension of this range is dependent on the specific reaction conditions chosen for a particular polymerization.

In Fig. 25 termination and propagation rate coefficients of MA, DA, MMA, BMA, and DMA homopolymerizations are given for 40 °C and 1000 bar on a double-log scale. High-pressure k_p and k_t data is plotted as the entire set of SP–PLP experiments has been carried out under these conditions.

The family type behavior of k_p (Section 2) is seen for the methacrylates and also for the acrylates. For k_t, however, no such family type behavior occurs. k_t of MA is by almost two orders of magnitude above k_t of DA. A significantly higher k_t is also found for MMA as compared to DMA. Interestingly, the k_ts of the two-dodecyl esters, DA and DMA, are more or less identical.

Copolymerization k_t studies should be helpful for the understanding of the large differences in homopolymerization k_t. Moreover, copolymerizations are technically relevant reactions and any improvement in the modeling of copolymerization k_t behavior is important. Among the binary systems that may be prepared from of the monomers contained in Fig. 25, the systems DA–MA and DA–DMA

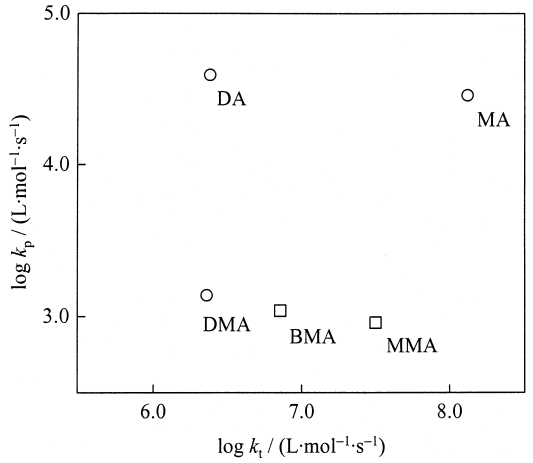

Fig. 25. Propagation rate coefficients k_p and termination rate coefficients k_t for several acrylates and methacrylates at 40 °C and 1000 bar, for which copolymerization studies will be reported. Reproduced with permission from Macromolecules 1999;32:1445. © 1999 American Chemical Society [142].

are of particular interest. The homopolymerization k_ps of MA and DA are almost the same, whereas the k_ts are significantly apart, by a factor of 55. With DA–DMA, on the other hand, the homo-k_ts are more or less identical and the homo-k_ps are clearly different. The copolymerization k_ts are deduced from SP–PLP $(k_p/k_t)_{copo}$ data that are combined with $k_{p,copo}$ from separate copolymerization PLP–SEC experiments which were also carried out at 40 °C and 1000 bar (Section 2.3.2).

The resulting $k_{t,copo}$ values are plotted together with the homopolymerization values in Fig. 26. The correlation of log $k_{t,copo}$ with f_{DA}, the mole fraction of DA in the monomer mixture, closely fits to a straight line. This result is not overly surprising for the DA–DMA system where the two homo-termination rate coefficients are identical, but is noteworthy for DA–MA where the homo-k_ts differ by almost two orders of magnitude.

As is demonstrated in Ref. [142], among the existing models for $k_{t,copo}$ which are presented and discussed in the Fukuda et al. [153] paper, only the penultimate-type model given in Eq. (36) allows for an adequate fit of the measured $k_{t,copo}$ data for both DA–MA and DA–DMA

$$k_{t,copo}^{0.5} = k_{t11,11}^{0.5} P_{11} + k_{t21,21}^{0.5} P_{21} + k_{t22,22}^{0.5} P_{22} + k_{t12,12}^{0.5} P_{12} \tag{36}$$

As with free-radical propagation in binary copolymerizations, in addition to the terminal unit, the penultimate unit at the free-radical terminus is considered in modeling $k_{t,copo}$. This approach has first been used by Russo and Munari [154,155]. The k_t penultimate model is associated with a significantly enhanced number of individual termination rate coefficients. Given in Eq. (37) is the general expression for penultimate model $k_{t,copo}$ in binary copolymerizations

$$k_{t,copo} = \sum_{l=1}^{2} \sum_{k=1}^{2} \sum_{i=1}^{2} \sum_{j=1}^{2} P_{ij} P_{kl} k_{tij,kl} \tag{37}$$

$k_{t,copo}$ is composed of ten individual termination rate coefficients, $k_{tij,kl}$, which refer to the reaction of two radicals with specified terminal units ij and kl, respectively. The P_{ij}s and P_{kl}s indicate the relative

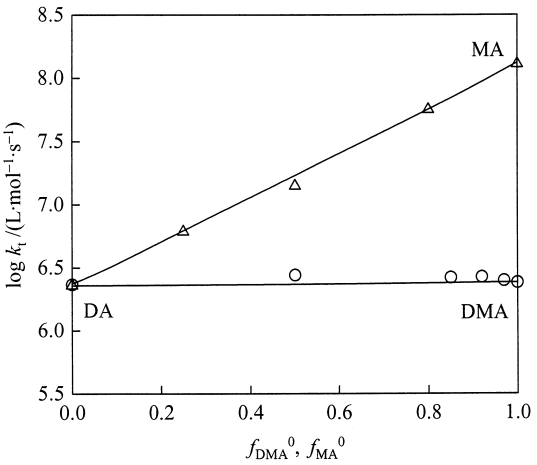

Fig. 26. Termination rate coefficients (in the plateau region, see text) of DA–MA and DA–DMA copolymerizations at 40 °C and 1000 bar, plotted against the (initial) mole fraction of either MA or DMA, respectively. Reproduced with permission from Macromolecules 1999;32:1445. © 1999 American Chemical Society [142].

populations of the four types of 'penultimate' free radicals, with chain ends *ii*, *ij*, *jj*, or *ji*. These populations may be calculated from the propagation rate coefficients and reactivity ratios [156]. The relatively large number of termination rate coefficients, $k_{tij,kl}$, is reduced by replacing the 'unlike' coefficients, $k_{tij,kl}$ with *ij* being different from *kl*, by the associated coefficients for termination of 'like' radicals, $k_{tij,ij}$ and $k_{tkl,kl}$, via the geometric mean approximation (Eq. (38)):

$$k_{tij,kl} = (k_{tij,ij} k_{tkl,kl})^{0.5} \tag{38}$$

Eq. (38) is the expression used by Fukuda et al. [153] whereas in Russo and Munari's original paper an additional factor of 2 is contained on the RHS of Eq. (38). It should be noted that geometric mean expressions, such as Eq. (38), are used in gas kinetic studies to estimate cross-termination [157]. The elimination of 'unlike' termination rate coefficients $k_{tij,kl}$ by the 'like' ones, $k_{tij,ij}$ and $k_{tkl,kl}$ reduces the number of penultimate-unit termination rate coefficients from ten to four. Eq. (38) in conjunction with Eq. (37) yields Eq. (36) which, as has already been pointed out, allows for a very satisfactory representation of $k_{t,copo}$ in the DA–DMA and DA–MA systems.

The close-to-linear correlation of log $k_{t,copo}$ vs. f data observed for monomers belonging to the same family, MA and DA, suggests to try corresponding plots for other systems. As is shown in Ref. [142], the Ito and O'Driscoll $k_{t,copo}$ data for MMA–BMA and MMA–DMA at 30 °C and ambient pressure [158], which were deduced from rotating sector experiments, indeed closely fit to linear log $k_{t,copo}$ vs. f relations.

The data in Fig. 26 together with the corresponding plots for MMA–BMA and MMA–DMA [142] may suggest that $k_{t,copo}$ might generally be accessible from homo-termination data via linear log $k_{t,copo}$ vs. f correlations. That this is not the case, is clearly seen from data for several binary systems presented in the Fukuda et al. [153] paper and has recently been demonstrated by Feldermann with SP–PLP experiments carried out on the MA–DMA system [135,159].

Plotted in Fig. 27 is $k_{t,copo}$ for the MA–DMA and the MA–DA systems as a function of the

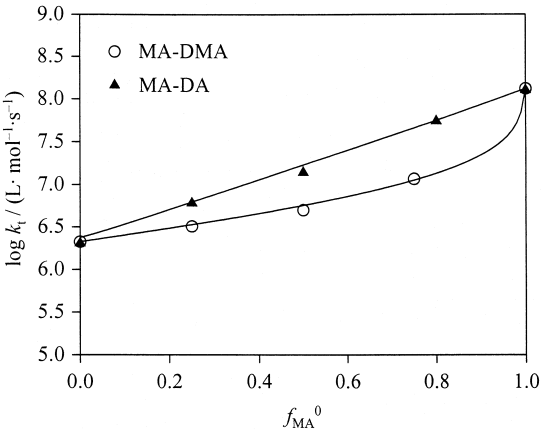

Fig. 27. Termination rate coefficients (in the plateau region, see text) of MA–DA and MA–DMA copolymerizations at 40 °C and 1000 bar, plotted against the (initial) mole fraction of MA [135,142].

MA mole fraction of the (initial) monomer mixture. The data refers to polymerization conditions of 1000 bar and 40 °C. The two systems are interesting in that $k_{t,copo}$ varies in between limiting homo-termination rate coefficients of the same size. In clear contrast to the MA–DA data which has already been shown in Fig. 26, MA–DMA $k_{t,copo}$ exhibits no linear log $k_{t,copo}$ vs. f correlation. The reason behind this is that, other than with the MA–DA system, the reactivity ratios of the MA–DMA system clearly differ from unity ($r_{MA} = 0.38$ and $r_{DMA} = 2.07$). As a consequence, the populations of the different types of free radicals are not related to the monomer mole fraction in a simple way. Actually, the fraction of free radicals with a DMA terminus is significantly higher than the DMA monomer mole fraction which results in $k_{t,copo}$ being shifted toward the lower homo-k_t value of DMA. The penultimate-type model (Eq. (36)) takes the actual populations properly into account and thus is capable of fitting also the MA–DMA $k_{t,copo}$ data. Actually, the line through the MA–DMA data is a fit to Eq. (36).

The underlying penultimate $k_{t,copo}$ model with the geometric mean approximation (Eq. (38)) being used to eliminate the 'unlike' termination rate coefficients, $k_{tij,kl}$, allows for a satisfactory fit of the experimental material that is presently available for the initial plateau region of (meth)acrylate copolymerizations. Arguments for the excellent representation of $k_{t,copo}$ data via Eq. (36) have been considered in Ref. [142]. It certainly comes as a surprise that within the partly rather extended plateau $k_{t,copo}$ regions, up to 50 or even more percent monomer conversion, termination rate of macroradicals may be best fitted by a model that only considers the two terminal units of each of the reacting monomers. The strongest argument in favor of such a k_t penultimate model assigns control of the termination reaction to steric (entropic) factors and thus to shielding effects at the free-radical chain-end. Substituents on the terminal and on the penultimate unit should (primarily) contribute to this shielding. Steric shielding would easily explain the trends seen in the homo-k_ts of (meth)acrylates in the initial plateau region (Fig. 25). k_t should strongly increase in going from the dodecyl to the methyl members in the (meth)acrylate families. Moreover, the dominant shielding effect which must be expected to occur with the dodecyl monomers explains the minor difference in k_t between DA and DMA. The poor shielding conditions with the methyl members of both families give rise to a significant

lowering of k_t upon the addition of the α-methyl group, that is in going from MA to MMA. This is indeed what Fig. 25 shows.

A particularly strong argument in favor of segmental reorientation under steric control by the substituents at the free-radical chain end being responsible for the plateau regions comes from the obvious success of the geometric mean approximation in replacing termination rate coefficients of two radicals with 'unlike' penultimate units by the corresponding 'like' coefficients (Eq. (38)). The successful application of Eq. (36), of course, does not prove that it is definitely only the last two units on the radical terminus which contribute to the shielding effect. It appears, however, that consideration of these two units accounts for most of the effect.

The shielding argument also offers a convincing explanation for the plateau behavior of k_t in the initial conversion range where bulk viscosity and thus center-of-mass diffusion of macroradicals significantly increase with conversion. It may also be easily understood that no such initial plateau region of constant k_t is seen with the ethene homopolymerization (Fig. 18). Steric effects also explain why highly substituted monomers such as itaconates [160–162] and fumarates [163,164] exhibit particularly low k_t. Finally, the steric argument is fully consistent with the observation made, e.g. within the methacrylate family (Fig. 25) that toward larger steric hindrance the plateau region of constant k_t is enhanced.

The initial plateau region in bulk homopolymerizations thus appears to be best understood in terms of segmental reorientation occurring in the intra-coil environment which primarily consists of the monomer. This process, which controls termination at low and moderate degrees of monomer conversion in bulk polymerizations of (meth)acrylates and of many other types of monomers, is insensitive toward bulk viscosity, but may be affected by low molecular weight materials, in particular by solvent species. Solvent materials may vary the intra-coil viscosity and, as a consequence, may influence segmental mobility. The impact of solvent effects on the size of the plateau k_t value is made particularly clear by systematic studies of Fischer et al. [165] into MMA solution polymerizations. They showed that the variation of solution viscosity, measured *prior* to polymerization, scales inversely with the size of the plateau k_t value. SP–PLP experiments in solution of supercritical CO_2 also reveal substantial solvent effects on k_t (Section 3.6).

With respect to modeling copolymerization k_t, particular interest relates to the linear correlation of log k_t vs. the monomer mole fraction that has been observed for mixtures of monomers belonging to the same family, e.g. both monomers are alkyl acrylates as in Fig. 26. The associated formula for $k_{t,copo}$ of such binary copolymerizations reads

$$\log k_{t,copo} = f_1 \log k_{t,1} + f_2 \log k_{t,2} \tag{39}$$

where $k_{t,1}$ and $k_{t,2}$ are the homo-termination rate coefficients of monomers 1 and 2, respectively (both referring to T and p of the copolymerization experiment). As a further test of this remarkably simple family type behavior of $k_{t,copo}$, SP–PLP experiments have been carried out on the two ternary systems MA–BA–DA and MMA–BMA–DMA with the investigations again being restricted to the initial plateau region in which the same type of k_t-controlling mechanism should apply [150].

By analogy to Eq. (39), the following expression is assumed to hold for terpolymerization $k_{t,terpo}$

$$\log k_{t,terpo} = f_1 \log k_{t,1} + f_2 \log k_{t,2} + f_3 \log k_{t,3} \tag{40}$$

where $f_1 + f_2 + f_3 = 1$ and $k_{t,3}$ is the homo-termination rate coefficient of the third monomer.

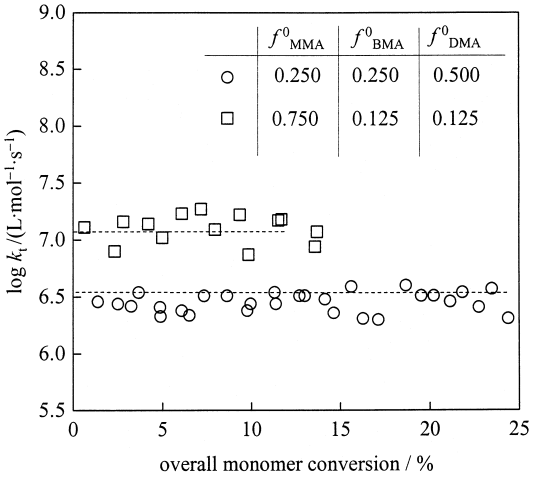

Fig. 28. Termination rate coefficients for two terpolymerizations of MMA, BMA, and DMA at 40 °C and 1000 bar plotted as a function of overall monomer conversion. The initial methacrylate mole fractions, f_i^0, are given in the figure. Reproduced with permission from Macromol Chem Phys 1999;200:1764. © 1999 Wiley–VCH [150].

Each of the two terpolymerizations is assumed to be close to ideal with no significant changes in composition of the monomer mixture, at least not during the reaction up to overall monomer conversions of about 30%. Another important advantage of these particular systems relates to the fact that the terpolymerizing monomers exhibit a pronounced family type behavior of k_p which allows for reasonable estimates of terpolymerization k_p via the IPUE model [150]. $k_{p,terpo}$ is required in order to calculate $k_{t,terpo}$ from $(k_t/k_p)_{terpo}$ which is the primary experimental quantity from SP–PLP. Actually, for the estimate of $k_{p,terpo}$, the simplified IPUE model (which assumes r_1r_2 to be close to s_1s_2) has been used twice. In a first step, the monomers which are similar in ester chain-length, MA + BA and MMA + BMA, are coupled, via the IPUE model, to generate a pseudo-monomer component that reflects the relative concentration of these two monomers. Within a further IPUE procedure, this pseudo-monomer is combined with the third monomer, DA or DMA, to yield $k_{p,terpo}$ for a pre-selected monomer mixture. In view of the large differences in k_t between the members of each family, the uncertainties associated with this estimate of $k_{p,terpo}$ will not seriously affect the resulting terpolymerization k_t values.

Shown in Fig. 28 are terpolymerization k_t data for two monomer mixtures prepared from MMA, BMA, and DMA at mole fractions of 0.250, 0.250, 0.500 (open circles) and 0.750, 0.125, 0.125 (open squares), respectively [150]. The dashed lines are $k_{t,terpo}$ data estimated from the very simple correlation (Eq. (40)) which requires only the knowledge of homopolymerization k_ts and of the (initial) monomer mole fractions, f_i^0, which to a good approximation hold for the entire plateau range. A very reasonable agreement between predicted and measured, via SP–PLP, k_t values is seen.

As is shown by a series of experiments in Ref. [150], $k_{t,terpo}$ of ternary mixtures composed of MA, BA, and DA may also be accurately predicted via Eq. (40) on the basis of known homo-k_t values and reactivity ratios. This observation has far-reaching consequences for the simulation of polymerization kinetics in ternary free-radical polymerizations of monomers that belong to the same family. In copolymerization and terpolymerization systems where the binary reactivity ratios clearly differ from unity, modeling has to be carried out via Eq. (36). The more or less linear log $k_{t,copo}$ vs. f correlation will be

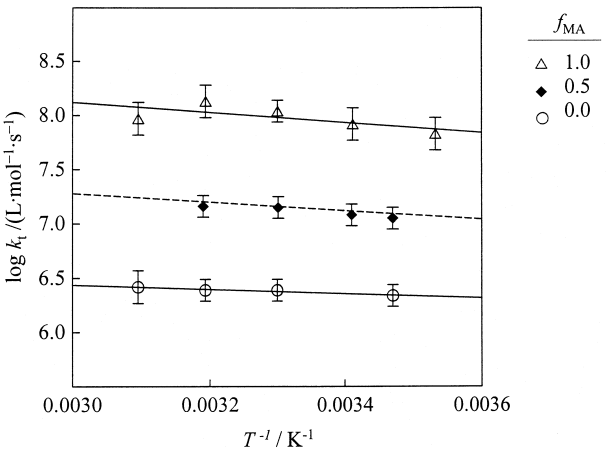

Fig. 29. Temperature dependence of the termination rate coefficient (in the plateau region, see text) for MA and DA homo- and copolymerizations at 1000 bar.

restricted to systems where the mole fraction of monomer *i*, to a good approximation, scales with the concentration of free radicals terminating in the associated unit *i*. The simple linear dependence is probably due to the fact that both the steric crowding, which results from substituents at the free-radical terminus, and the viscosity of the monomer mixture exhibit such a logarithmic dependence on mole fractions.

To summarize, Eqs. (39) and (40) are very useful for estimating copolymerization and terpolymerization k_t of monomers with reactivity ratios close to unity as within the alkyl acrylate or the alkyl methacrylate family. With the exception of the minor influences resulting from the chain-length dependence of k_t, the two equations account for the major impact of composition on $k_{t,copo}$ and on $k_{t,terpo}$. It needs to remembered that these predictions of k_t are limited to the initial plateau region of bulk polymerizations which, however, may be fairly extended, e.g. up to 50% monomer conversion in systems containing significant fractions of DA or of DMA.

3.5. Pressure and temperature dependence of copolymerization k_t

Linear dependencies of log k_t vs. monomer mole fraction that hold within individual monomer families have been illustrated taking data for 40 °C and 1000 bar as an example. These simple (intra-family) correlations also hold at other temperature and pressure conditions, as has been demonstrated by Külpmann [148] with a series of MA–DA copolymerizations at temperatures between 10 and 40 °C and pressures from 10 to 2000 bar. Results of this study are presented in Figs. 29 and 30. The dashed lines represent estimates, via Eq. (39), of the copolymerization termination rate coefficient for $f_{MA} = f_{DA} = 0.5$ from the associated homo-termination rate coefficients at identical T and p. The experimental $k_{t,copo}$ data measured for MA–DA copolymerizations ($f_{MA} = 0.5$) at 1000 bar and several temperatures (full symbols in Fig. 29) are in excellent agreement with the predicted numbers. The $k_{t,copo}$ data at 40 °C and pressure variation, shown in Fig. 30, are consistent with the finding from Fig. 29. The predicted $k_{t,copo}$ data are in reasonable agreement with the measured values.

Further SP–PLP studies into $k_{t,copo}$ at p and T variation should be carried out on monomer mixtures

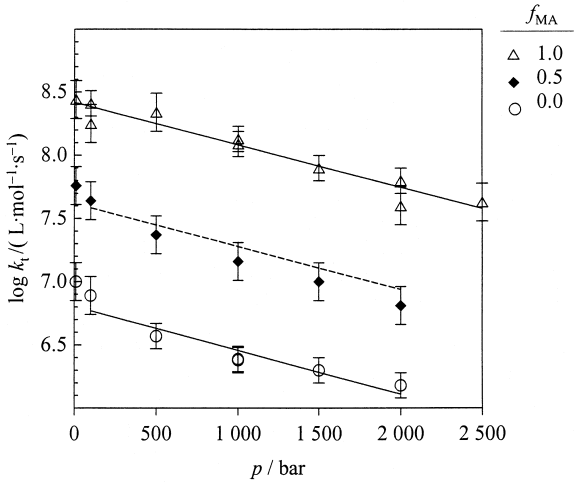

Fig. 30. Pressure dependence of the termination rate coefficient (in the plateau region, see text) for MA and DA homo- and copolymerizations at 40 °C.

which do not belong to the same family. Moreover, such investigations should be extended to conversion regions where, for one or for both monomers, mechanisms other than segmental diffusion control termination rate.

3.6. Termination rate coefficients in solution

Because of the superior quality by which SP–PLP signals may be recorded for acrylate monomers, in particular for DA, pulsed-laser induced studies into the solvent influence on k_t have primarily been carried out for acrylates. In order to detect potential solvent effects, the solvent should not be too similar to the monomer. CO_2 perfectly meets this requirement in that it is an unusual solvent which, with respect to polarity and viscosity, is significantly different from the acrylate monomers and from other conventional solvents used in acrylate polymerization.

Fig. 31 shows the comparison of k_t values which have been obtained in bulk and in solution (containing approximately 40 wt% CO_2) homopolymerizations of MA and DA [166]. The k_t data are only given for the plateau region (of bulk polymerization), which with MA extends up to about 20%, but with DA up to about 50%. Two interesting observations can be made from this data: (1) With MA practically no difference in k_t between bulk and solution data is seen whereas with DA the k_t plateau data in scCO_2 are by about a factor of eight above the bulk k_t values. (2) The DA situation is interesting in that bulk viscosity, which largely changes during the course of the reaction, does not affect bulk k_t, but the addition of CO_2 significantly changes k_t.

The observations in Fig. 31 are at least qualitatively consistent with the arguments on diffusion control of plateau k_t by segmental diffusion which depends on intra-coil viscosity, on steric effects at the free-radical terminus, and presumably also on the type of diffusing polymer segments. In case of DA, the steric hindrance plays a major role. As a consequence, the lowering of intra-coil viscosity, by adding CO_2, enhances the collision frequency of chain ends of entangled macroradicals and thereby increases termination rate. With MA, the impact of shielding effects on k_t is less pronounced and a high(er)

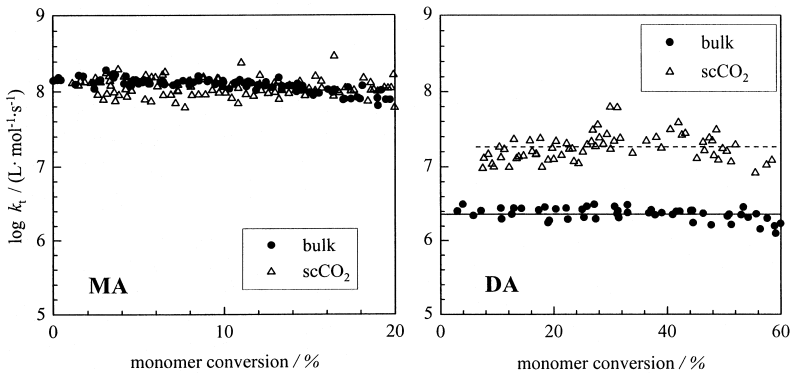

Fig. 31. Conversion dependence of k_t for bulk and solution ($scCO_2$) polymerizations of MA (left) and DA (right) at 40 °C and 1000 bar. Open markers refer to reactions in 40 wt% of CO_2 and filled markers to the bulk experiments [166].

fraction of free-radical chain-end collisions will be successful in bulk polymerization. Thus the enhanced mobility associated with the addition of CO_2 will not result in a significant enhancement of k_t.

For a quantitative description of the size of k_t, dynamic information from independent sources, e.g. on the viscosity of monomer–CO_2 mixtures, is required. Other than with the homopolymerizations, where the intra-coil environment is made up essentially of the monomer and thus stays constant over an initial conversion region, the composition of low molecular weight species changes in monomer–solvent polymerizations. In cases where such a reaction-induced change is associated with a major variation in viscosity, also k_t may vary. In situations where CO_2 is the solvent and where viscosity contributes to k_t control, as with DA, the decrease in viscosity within the initial polymerization period should result in an increase in k_t. A very weak indication of such an effect may be contained in the data in Fig. 31, but cannot be safely established. Comparison of the bulk and solution (in 46 wt% CO_2) k_t data of BA in Fig. 32 shows such an increase [143]. It is, however, by no means clear whether a change in viscosity of the monomer–solvent mixture contributes to this behavior or whether the initial increase, which is also (weakly) seen in bulk polymerization (Fig. 32), results from other effects which may be specific for BA.

PS–PLP studies into MMA polymerization in solution of toluene and of 2-butanone [137] (also) yield a linear dependence of log k_t on monomer mole fraction. The observed variation in k_t is small, but is larger than expected from estimated changes in the viscosity of the monomer mixture. It may not be ruled out that differences in free-radical chain-length may contribute to the measured small effects.

3.7. Chain-length dependence of k_t

Investigations into the chain-length dependence of termination rate coefficients are of fundamental interest, but may also be of practical relevance with respect to a full understanding and accurate modeling of free-radical polymerization processes. Several groups have addressed this issue during recent years [167–174]. It is beyond the scope of this article to refer to the field in any detail. Excellent surveys on the relevant literature have been provided by Litvinenko and Kaminsky [175] and recently by deKock et al. [10,11]. SP–PLP experiments are particularly well suited for investigations into the

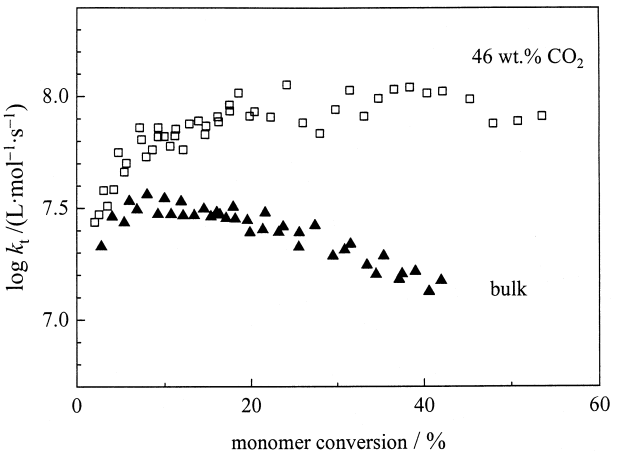

Fig. 32. Conversion dependence of k_t for BA polymerizations at 40 °C and 1000 bar. Open markers refer to reactions in 46 wt% of CO_2 and filled markers to the bulk experiments [143].

chain-length dependence of k_t. The Olaj group [13,14] and also deKock [10] deduced detailed information about k_t from analysis of MWD obtained under polymerization conditions that are close to single pulse initiation. Such MWD-based studies are not easily carried out at elevated degrees of monomer conversion. It appeared interesting to apply the SP–PLP technique toward investigations into k_t as a function of chain-length (CL), as this method may be used up to higher degrees of monomer conversion.

The time-resolved monomer conversion vs. time trace, measured after application of a laser single pulse, reflects the reactions of an almost mono-disperse free-radical population, the CL of which increases linearly with time t. As has been noted above, this simple CL vs. time correlation is the particularly attractive feature of an SP–PLP experiment. Due to non-synchronous propagation of individual free radicals, the CL distribution is slightly (Poisson) broadened and, as a consequence of transfer to monomer (and to polymer) reactions, the almost linear CL vs. t correlation is lost at larger t.

The model-free determination, via SP–PLP, of k_t as a function of CL proceeds via second derivatives of experimental $c_M(t)$ data [10]. At present, the signal-to-noise quality of SP–PLP data is insufficient for a reasonable estimate of such second derivatives. Thus, model expressions have been introduced to account for a CL dependence of termination rate. Eq. (41) applies to termination of two free radicals, each of chain length i (as in SP–PLP),

$$k_t(i,i) = 2k_t(1,1)\frac{1}{i^{\alpha}} \tag{41}$$

where $k_t(1,1)$ is the termination rate coefficient of two small free radicals and the exponent α represents the extent of CL dependence. α has been reported to be close to 0.2 in the initial period of styrene [13,14,171] and methyl methacrylate [13,14,171] polymerizations, but also somewhat higher values can be found in the literature [10]. In his pioneering SP–PLP study, Schweer deduced an exponent of $\alpha = 0.2 \pm 0.1$ for the high-pressure, high-temperature ethene polymerization at monomer conversions of about 10% [78].

During her SP–PLP studies into methyl and dodecyl acrylate bulk polymerization kinetics, Kurz

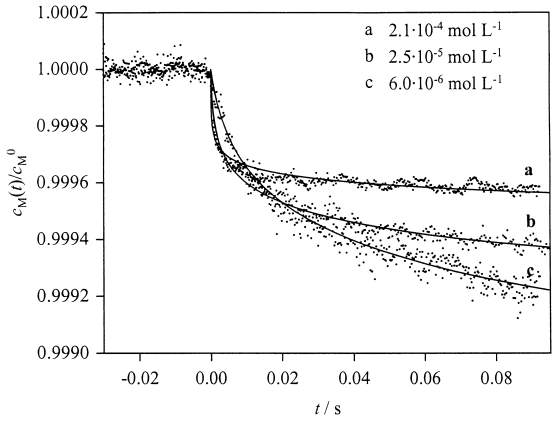

Fig. 33. Relative monomer concentration vs. time trace of methyl acrylate homopolymerizations at 40 °C and 1000 bar carried out at different levels of primary free-radical concentration (a–c) as given in the figure [176]. The full lines are obtained from fitting the data to Eq. (20). For details see text. Reproduced with permission from Macromol Theory Simul 2000;9:442. © 2000 Wiley–VCH.

[134] observed that k_t depends on c_R^0, the concentration of primary radicals generated by a SP. An increase of k_t with c_R^0 was seen upon either increasing photo-initiator concentration or laser pulse energy. As a consequence of such an increase, the final degree of monomer conversion induced by a single pulse decreases toward higher c_R^0. Extended investigations into several monomer systems revealed that this very surprising result is observed whenever DMPA (2,2-dimethoxy-2-phenylacetophenone) is used as the photoinitiator in laser-induced free-radical polymerization [13,14,140,147,176].

The remarkable finding is illustrated in Fig. 33 by SP–PLP data measured at low monomer conversions (of approximately 2%) in methyl acrylate (MA) homopolymerizations at 40 °C and 1000 bar [176]. The traces are from experiments at three levels of initial DMPA concentration, between 5×10^{-2} and 5×10^{-4} mol l^{-1}. The laser energy per pulse has additionally been varied, between 0.5 and 4.5 mJ, to further enhance the range of initial free-radical concentration, which is between 2.1×10^{-4} and 6.0×10^{-6} mol l^{-1}. The three SP–PLP experiments have been carried out at otherwise identical conditions. As has been outlined in Ref. [176], the observed lowering of monomer conversion upon increasing c_R^0 cannot be explained by ideal SP–PLP kinetics. The puzzling behavior is related to the peculiarities of photo-induced DMPA decomposition which has been studied in detail by Fischer et al. [177]. Among the two free radicals produced from DMPA, $PhCO^{\cdot}$ and $Ph(OCH_3)_2C^{\cdot}$, without photochemical excitation, as in the SP–PLP experiment after application of the laser, the latter radical is not capable of starting macromolecular growth, but will be involved in termination reactions. The enhancement of DMPA decomposition thus is associated with both an increase in propagating and in terminating (inhibiting) free radicals. The chain-terminating potential of $Ph(OCH_3)_2C^{\cdot}$ radicals may account for the observed increase in k_t toward higher DMPA decomposition rate.

Simulations via the program package PREDICI® demonstrate that implementing this assumption of two types of primary free radicals, with only one of them being capable of reacting with a monomer molecule, cannot explain the experimental observations unless, in addition, the termination rate coefficient is considered to be chain-length dependent. The same result has been obtained from a recent study in which a reasonably reduced set of kinetic equations has been analytically solved [178]. The analysis

shows that the crossing of the time-resolved SP–PLP signals (e.g. as shown in Fig. 33) occurs whenever the two types of primary free radicals differ largely in their tendency to add to a monomer molecule and, at the same time, the termination rate coefficient is chain-length dependent. This finding opens up a novel route to deduce the CL dependence of k_t from SP–PLP experiments. Using widely different photo-initiator concentrations or laser pulse intensities in experiments with DMPA or with another initiator that photo-decomposes into two primary free radicals of quite different reactivity toward the monomer, provides monomer conversion vs. time curves from which, e.g. via PREDICI® modeling, the exponent α for CL dependent k_t may be deduced.

The novel procedure has been applied to several monomers [10,176]. Interestingly, two types of CL dependence have been found, a rather weak one with styrene and with methyl methacrylate, where α is approximately 0.15 ± 0.04, and a somewhat stronger one with methyl acrylate and with dodecyl acrylate where α is around 0.32 ± 0.04. A satisfactory explanation for this difference in the extent of CL dependence of k_t cannot yet be given. Khokhlov [179] pointed out that for chemically controlled reactions of macromolecular species, the chain-length dependence (according to Eq. (41)) of rate coefficients is adequately represented by an exponent of $\alpha = 0.16$ in case of reaction between functional groups at chain ends. The exponent is close to 0.28 in cases where one reactive site is at a chain end and the other is situated somewhere along the chain of the other species. For reaction between two species with both reactive sites being located somewhere along the chain, the exponent is even further enhanced ($\alpha = 0.43$). It cannot be ruled out that arguments along these lines may also apply to termination in free-radical polymerizations where steric hindrance may lead to some kind of chemical control instead of 'simple' diffusion control. Within such a picture, the larger value of the exponent α observed with the acrylates might indicate significant chain transfer activity in these materials. At present, however, no firm conclusion about such effects may be drawn and further systematic studies are required to resolve the origin of the different extents of CL dependence of k_t.

The exponent α deduced from the novel method for styrene and for MMA ($\alpha = 0.15 \pm 0.04$) is in close agreement with literature values from experimental studies into α of styrene: 0.17 (Olaj [13,14]), and 0.24 (Mahabadi [180]) and of MMA: 0.15. DeKock [10] reported α values for methyl acrylate, ethyl acrylate, and butyl acrylate for separate ranges of free-radical chain length, from 6 to 10, 15 to 30, and 50 to 100. Only the α values reported for the latter range are suitable for comparison with the results from SP–PLP. The α values determined by deKock are 0.35 ± 0.05 for MA, 0.35 ± 0.03 for ethyl acrylate, and 0.17 ± 0.03 for butyl acrylate. They are in close agreement with the acrylate α values from the SP–PLP studies carried out at different DMPA photo-initiator levels.

The presently available results indicate that the CLD of k_t is relatively weak for styrene and MMA and is stronger for MA and for other acrylates. All this data refers to the initial range of monomer conversion which may, however, be fairly extended, e.g. with dodecyl acrylate. The novel type of SP–PLP experiments, at substantial variation of DMPA concentration, have not yet been extended to higher conversion in MMA and styrene homopolymerization where k_t enormously decreases. It is of particular interest to identify the type and extent of CL dependence of k_t under conditions where center-of-mass diffusion is rate controlling.

Once k_t is known as a function of CL within wide ranges of polymerization conditions, the detailed CL dependent k_ts have to be used in conjunction with the actual size distribution of free radicals to estimate overall k_t for comparison with the average k_t values deduced from conventional kinetic analysis.

4. Conclusions

Pulsed laser techniques have enormously improved the quality by which rate coefficients of individual steps in free-radical polymerization may be measured. The PLP–SEC method is applicable to a wide variety of homopolymerizations and copolymerizations in homogeneous phase, either in bulk or in solution, with the limitations being especially due to the accurate determination of the MWD, at least in the region where the PLP structure occurs.

The SP–PLP method allows for a very detailed insight into homo- and copolymerization k_t as a function of temperature, pressure, monomer conversion, solvent concentration, and partly also of chain length. It appears to be a matter of priority to further enhance the signal quality of SP–PLP traces to make the method even more widely applicable.

References

[1] Brandrup A, Immergut EH, editors. Polymer handbook 3rd ed. New York: Wiley-Interscience, 1989.
[2] Deibert S, Bandermann E, Schweer J, Sarnecki J. Makromol Chem Rapid Commun 1992;13:351.
[3] van Herk AM, de Brouwer H, Manders BG, Luthjens LH, Hom ML, Hummel A. Macromolecules 1996;29:1027.
[4] German AL, Manders BG, Zirkzee H, Klumperman B, van Herk AM. Macromol Symp 1996;111:107.
[5] Aleksandrov AP, Genkin VN, Kitai MS, Smirnova IM, Sokolov VV. Sov J Quant Electron 1977;5:547.
[6] Olaj OF, Bitai I, Hinkelmann F. Makromol Chem 1987;188:1689.
[7] Olaj OF, Schnöll-Bitai I. Eur Polym J 1989;25:635.
[8] Buback M, Hippler H, Schweer J, Vögele H-P. Makromol Chem Rapid Commun 1986;7:261.
[9] Olaj OF, Vana P, Kornherr A, Zifferer G. Macromol Chem Phys 1999;200:2031.
[10] deKock JBL. PhD Thesis. Eindhoven; 1999.
[11] deKock JBL, van Herk AM, German AL. Submitted for publication.
[12] Deady M, Mau AWH, Moad G, Spurling TH. Makromol Chem 1993;194:1691.
[13] Olaj OF, Vana P. Macromol Rapid Commun 1998;19:433.
[14] Olaj OF, Vana P. Macromol Rapid Commun 1998;19:533.
[15] Olaj OF, Vana P. J Polym Sci, Polym Chem Ed 2000;38:697.
[16] Hutchinson RA, Paquet Jr. DA, McMinn JH. Macromolecules 1995;28:5655.
[17] Buback M, Busch M, Lämmel RA. Macromol Theor Simul 1996;5:845.
[18] Wulkow M. Macromol Theor Simul 1996;5:393.
[19] Bergert U, Beuermann S, Buback M, Kurz CH, Russell GT, Schmaltz C. Macromol Rapid Commun 1995;16:425.
[20] Beuermann S, Buback M, Davis TP, Gilbert RG, Hutchinson RA, Olaj OF, Russell GT, Schweer J, van Herk AM. Macromol Chem Phys 1997;198:1545.
[21] Beuermann S, Buback M, Davis TP, Gilbert RG, Hutchinson RA, Kajiwara A, Klumperman B, Russell GT. Macromol Chem Phys 2000;201:1355.
[22] Buback M, Gilbert RG, Hutchinson RA, Klumperman B, Kuchta FD, Manders BG, O'Driscoll KF, Russell GT, Schweer J. Macromol Chem Phys 1995;196:3267.
[23] Lämmel RA. PhD Thesis. Göttingen; 1996.
[24] Benoit H, Grubisic Z, Rempp P, Decker D, Zilliox JG. J Chim Phys 1996;63:1507.
[25] Buback M, Geers U, Kurz CH, Heyne J. Macromol Chem Phys 1997;198:3451.
[26] Jackson C, Chen Y-J, Mays JW. J Appl Polym Sci 1996;61:865.
[27] Zammit MD, Coote ML, Davis TP, Willett GD. Macromolecules 1998;31:955.
[28] McEwen CN, Jackson C, Larsen BS. Int J Mass Spectrom 1997;160:387.
[29] Montaudo MS. Macromol Symp 1999;141:95.
[30] Sarnecki J, Schweer J. Macromolecules 1995;28:4080.
[31] Bandermann F, Günther C, Schweer J. Macromol Chem Phys 1996;197:1055.
[32] Beuermann S, Paquet Jr. DA, McMinn JH, Hutchinson RA. Macromolecules 1996;29:4206.

[33] Buback M, Kuchta FD. Macromol Chem Phys 1995;196:1887.
[34] Zammit MD, Davis TP, Willett GD, O'Driscoll KF. J Polym Sci, Polym Chem 1997;35:2311.
[35] Coote ML, Davis TP. Macromolecules 1999;32:4290.
[36] van Herk AM, Manders BG, Canelas D, Quadir M, DeSimone JM. Macromolecules 1997;30:4780.
[37] Beuermann S, Buback M, Isemer C, Lacík I, Wahl A. Submitted for publication.
[38] Olaj OF, Schnöll-Bitai I. Monatshefte für Chemie 1999;130:731.
[39] O'Driscoll KF, Monteiro MJ, Klumperman B. J Polym Sci, Polym Chem Ed 1997;53:515.
[40] Coote ML, Davis TP. Eur Polym J 2000;36:2423.
[41] Beuermann S, Buback M, Russell GT. Macromol Rapid Commun 1994;15:351.
[42] Beuermann S, Buback M, Russell GT. Macromol Rapid Commun 1994;15:647.
[43] Quadir M, DeSimone JM, van Herk AM, German AL. Macromolecules 1998;31:6481.
[44] Beuermann S, Buback M, Kuchta FD, Schmaltz C. Macromol Chem Phys 1998;199:1209.
[45] Morrison BR, Piton MC, Winnik MA, Gilbert RG, Napper DH. Macromolecules 1993;26:4368.
[46] Hutchinson RA, Paquet Jr. DA, McMinn JH, Fuller RE. Macromolecules 1995;28:4023.
[47] Klumperman B, van Herk AM. In preparation.
[48] Hutchinson RA, Paquet Jr. DA, Beuermann S, McMinn JH. Ind Engng Chem Res 1998;37:3567.
[49] Muratore LM, Coote ML, Davis TP. Polymer 2000;41:1441.
[50] Shipp DA, Smith TA, Solomon DH, Moad G. Macromol Rapid Commun 1995;16:837.
[51] Beuermann S, Paquet Jr. DA, McMinn JH, Hutchinson RA. Macromolecules 1997;30:194.
[52] Kuchta FD, van Herk AM, German AL. Macromolecules 2000;33:3641.
[53] Manders BG. PhD Thesis. Eindhoven; 1997.
[54] Buback M, Kurz CH, Schmaltz C. Macromol Chem Phys 1998;199:1721.
[55] Beuermann S, Buback M, El Rezzi V, Jürgens M, Nelke D. In preparation.
[56] Lyons RA, Hutovic J, Piton MC, Christie DI, Clay PA, Manders BG, Kable SH, Gilbert RG. Macromolecules 1996;29:1918.
[57] Beuermann S, Buback M, Schmaltz C. Macromolecules 1998;31:8069.
[58] Ganachaud F, Balic R, Monteiro MJ, Gilbert RG. Macromolecules 2000;33:8589.
[59] Lacík I, Beuermann S, Buback M. Macromolecules 2001;34:6224.
[60] Hutchinson RA, Richards JR, Aronson MT. Macromolecules 1994;27:4530.
[61] Hutchinson RA, Paquet Jr. DA, McMinn JH, Beuermann S, Fuller R, Jackson C. Fifth International Workshop on Polymer Reaction Engineering (DECHEMA Monographs 131). Weinheim: VCH; 1995.
[62] Beuermann S, Buback M, Nelke D. Macromolecules 2001;34:6637
[63] Balic R, Gilbert RG, Zammit MD, Davis TP, Miller C. Macromolecules 1997;30:3775.
[64] Hutchinson RA, Aronson MT, Richards JR. Macromolecules 1993;26:6410.
[65] Morrison DA, Davis TP. Macromol Chem Phys 2000;201:2128.
[66] Lachlan HY, Coote ML, Rodney PC, Davis TP. J Polym Sci, Polym Chem Ed 2000;38:2192.
[67] Hutchinson RA, Beuermann S, Paquet Jr. DA, McMinn JH. Macromolecules 1997;30:3490.
[68] Hutchinson RA, Beuermann S, Paquet Jr. DA, McMinn JH. Macromolecules 1998;31:1542.
[69] Buback M, Kurz CH. Macromol Chem Phys 1998;199:2301.
[70] Busch M, Wahl A. Macromol Theor Simul 1998;7:217.
[71] Britton D, Heatley F, Lovell PA. Macromolecules 1998;31:2828.
[72] Ahmed N, Heathly F, Lovell PA. Macromolecules 1998;31:2822.
[73] Plessis C, Arzamendi G, Leiza JR, Schoonbrood HAS, Charmont D, Asua JM. Macromolecules 2000;33:4.
[74] Azukizawa M, Yamada B, Hill DJT, Pomery P. Macromol Chem Phys 2000;201:774.
[75] Yamada B, Azukizawa M, Yamazoe H, Hill DJT, Pomery P. Polymer 2000;41:5611.
[76] van Herk AM. Macromol Theor Simul 2000;9:433.
[77] Buback M, Schweer J. Z Phys Chem NF 1989;161:153.
[78] Schweer J. PhD Thesis. Göttingen; 1988.
[79] Buback M. Macromol Symp 1996;111:229.
[80] Coote ML, Zammit MD, Davis TP, Willett GD. Macromolecules 1997;30:8182.
[81] Coote ML, Davis TP. Prog Polym Sci 1999;24:1217.
[82] Morris LM, Davis TP, Chaplin RP. Polymer 2001;42:941.

[83] Hutchinson RA, McMinn JH, Paquet Jr. DA, Beuermann S, Jackson C. Ind Engng Chem Res 1997;36:1103.
[84] Fukuda T, Ma Y-D, Inagaki H. Macromolecules 1985;18:17.
[85] Schweer J. Makromol Chem Theor Simul 1993;2:485.
[86] Fukuda T, Ma Y-D, Kubo M, Inagaki H. Macromolecules 1991;24:370.
[87] Olaj OF, Schnöll-Bitai I. Makromol Chem Rapid Commun 1990;11:459.
[88] Kukulj D, Davis TP. Macromolecules 1998;31:5668.
[89] Piton MC, Winnik MA, Davis TP, O'Driscoll KF. J Polym Sci, Part A: Polym Chem Ed 1990;28:2097.
[90] Coote CL, Davis TP. Macromolecules 1999;32:3626.
[91] Buback M, Feldermann A, Barner-Kowollik C, Lacík I. Macromolecules 2001;34:5439.
[92] Fukuda T, Ma Y-D, Kubo K, Takada A. Polym J (Tokyo) 1989;12:1003.
[93] van Herk AM, Dröge T. Macromol Theor Simul 1997;6:1263.
[94] Schoonbrood HAS, van den Reijen B, de Kock JBL, Manders BG, van Herk AM, German AL. Macromol Rapid Commun 1995;16:119.
[95] Coote ML, Davis TP. Polym React Engng 1999;7:363.
[96] Harwood HJ. Makromol Chem Macromol Symp 1987;10/11:331.
[97] Kamachi M. Adv Polym Sci 1981;38:55.
[98] Semchikov YD. Macromol Symp 1996;111:317.
[99] Kratochvil P, Straková D, Stejskal J, Tuzar Z. Macromolecules 1983;16:1136.
[100] Romack TJ, Maury EE, DeSimone JM. Macromolecules 1995;28:912.
[101] Kendall JL, Canelas DA, Young JL, DeSimone JM. Chem Rev 1999;99:543.
[102] Dionisio J, Mahabadi HK, O'Driscoll KF, Abuin E, Lissi EA. J Polym Sci, Polym Chem Ed 1979;17:1981.
[103] Kuchanov SI, Russo S. Macromolecules 1997;30:4511.
[104] Kazarian SG, Vincent MF, Bright FV, Liotta CL, Eckert CA. J Am Chem Soc 1996;118:1729.
[105] Kazarian SG, Brantley NH, West BL, Vincent MF, Eckert CA. Appl Spectrosc 1997;51:491.
[106] Rindfleisch F, DiNoia TP, McHugh MA. J Phys Chem 1996;100:15581.
[107] Ganachaud F, Monteiro MJ, Gilbert RG, Dourges M-A, Thang SH, Rizzardo E. Macromolecules 2000;33:6738.
[108] Brüssau R, Goetz N, Mächtle W, Stölting J. Tenside Surf Det 1991;28:396.
[109] Kilz P. Private communication.
[110] Clay PA, Gilbert RG. Macromolecules 1995;28:552.
[111] Heuts JPA, Kukulj D, Forster DJ, Davis TP. Macromolecules 1998;31:2894.
[112] Heuts JPA, Davis TP. Macromolecules 1999;32:6019.
[113] Moad G, Moad CL. Macromolecules 1996;29:7727.
[114] Beuermann S, Buback M, El Rezzi V. In preparation.
[115] Heuts JPA, Forster DJ, Davis TP, Yamada B, Yamazoe H, Azukizawa M. Macromolecules 1999;32:2511.
[116] Foster DJ, Heuts JPA, Lucien F, Davis TP. Macromolecules 1999;32:5514.
[117] Buback M, Lämmel RA. Macromol Theor Simul 1997;6:145.
[118] Henrici-Olivé G, Olivé S. Fortschr Hochpolym-Forsch 1961;2:496.
[119] Buback M, Lämmel RA. Macromol Theor Simul 1998;7:197.
[120] Beuermann S, Buback M. In: Matyaszewski K, editor. Controlled radical polymerization, ACS symposium series 685. Washington, DC: American Chemical Society, 1998. p. 84.
[121] Manders BG, van Herk AM, German AL, Sarnecki J, Schomäcker R, Schweer J. Makromol Chem Rapid Commun 1993;14:693.
[122] Jung M, van Hamersveld EMS, van Herk AM. Macromol Rapid Commun 2001;22:978.
[123] Schweer J, van Herk AM, Pijpers RJ, Manders BG, German AL. Macromol Symp 1995;92:31.
[124] Jung M, van Casteren I, Monteiro MJ, van Herk AM, German AL. Macromolecules 2000;33:3620.
[125] Shen J, Tian Y, Wang G, Yang M. Makromol Chem 1991;192:2669.
[126] Carswell TG, Hill DJT, Londero DI, O'Donnell JH, Pomery PJ, Winzor CL. Polymer 1992;33:137.
[127] Ballard MI, Gilbert RG, Napper DH, Pomery PJ, O'Sullivan PW, O'Donnell JH. Macromolecules 1986;19:1303.
[128] Buback M, Degener B, Huckestein B. Makromol Chem Rapid Commun 1989;10:311.
[129] Gridnev AA, Ittel SD. Macromolecules 1996;29:5864.
[130] Fischer H, Radan L. Angew Chem 2001;113:1380.
[131] Moad G, Rizzardo E, Solomon DH, Beckwith ALJ. Polym Bull 1992;29:647.

[132] Olaj OF, Vana P, Zoder M, Kornherr A, Zifferer G. Macromol Rapid Commun 2000;21:913.
[133] Buback M, Kowollik C. Macromolecules 1998;31:3211.
[134] Kurz CH. PhD Thesis. Göttingen; 1995.
[135] Feldermann, A. Diploma Thesis. Göttingen; 1999.
[136] Buback M, Huckestein L, Ludwig B. Makromol Chem Rapid Commun 1992;31:1.
[137] Beuermann S, Buback M, Russell GT. Macromol Chem Phys 1995;196:2493.
[138] Buback M, Kuchta F-D. Macromol Chem Phys 1997;198:1455.
[139] Buback M, Hinton C. Vibrational spectroscopy in dense fluid phases. In: Isaacs NS, Holzapfel WB, editors. High-pressure techniques in chemistry and physics: a practical approach. Oxford: Oxford University Press, 1997. p. 151.
[140] Kowollik C. PhD Thesis. Göttingen; 1999.
[141] Sack-Kouloumbris R, Meyerhoff G. Makromol Chem 1989;190:1133.
[142] Buback M, Kowollik C. Macromolecules 1999;32:1445.
[143] Beuermann S, Buback M, Schmaltz C. Ind Engng Chem Res 1999;38:3338.
[144] Buback M. Makromol Chem 1990;191:1575.
[145] Mähling FO, Klimesch R, Schwibach M, Buback M, Busch M. Chem Ing Technol 1999;71:1301.
[146] Beuermann S. PhD Thesis. Göttingen; 1993.
[147] Buback M, Kowollik C, Kurz CH, Wahl A. Macromol Chem Phys 2000;201:464.
[148] Külpmann A. Diploma Thesis. Göttingen; 2000; Buback M, Barner-Kowollik C, Kulpmann A. Submitted for publication.
[149] Buback M, Külpmann A, Kurz CH. In press.
[150] Buback M, Kowollik C. Macromol Chem Phys 1999;200:1764.
[151] Schmaltz C. Private communication. Göttingen; 1997.
[152] Bergert U. PhD Thesis. Göttingen; 1994.
[153] Fukuda T, Ide N, Ma Y-D. Macromol Symp 1996;111:305.
[154] Russo S, Munari SJ. Macromol Sci Chem 1968;2:1321.
[155] Bonta G, Gallo BM, Russo S. J Chem Soc Faraday Trans 1975;71:1727.
[156] Fukuda T, Kubo K, Ma Y. Prog Polym Sci 1992;17:875.
[157] Bayes KD, Garland LJ. J Phys Chem 1990;94:4941.
[158] O'Driscoll KF, Ito K. J Polym Sci 1979;17:3913.
[159] Buback M. Macromol Symp 2001;174:213.
[160] Matsumoto A, Yamagishi K, Otsu T. Eur Polym J 1995;31:121.
[161] Otsu T, Yamagishi K, Matsumoto A, Yoshioka M, Watanabe H. Macromolecules 1993;26:3026.
[162] Otsu T, Yamagishi K, Yoshioka M. Macromolecules 1992;25:2713.
[163] Matsumoto A, Otsu T. Macromol Symp 1995;98:139.
[164] Matsumoto A, Otsu T. Proc Jpn Acad B 1994;70:43.
[165] Fischer JP, Mücke G, Schulz GV. Ber Bunsenges physik Chem 1970;73:1077.
[166] Beuermann S, Buback M, Nelke D. In preparation.
[167] Olaj OF, Kornherr A, Zifferer G. Macromol Rapid Commun 1998;19:89.
[168] Olaj OF, Zifferer G, Gleixner G. Macromol Chem Rapid Commun 1985;6:773.
[169] Olaj OF, Zifferer G, Gleixner G. Makromol Chem 1986;187:977.
[170] Olaj OF, Zifferer G, Gleixner G. Macromolecules 1987;20:839.
[171] Mahabadi HK. Macromolecules 1991;24:606.
[172] Russell GT. Macromol Theor Simul 1995;4:519.
[173] Russell GT. Macromol Theor Simul 1995;4:497.
[174] Nikitin AN, Evseev AV. Macromol Theor Simul 1997;6:1191.
[175] Litvinenko GI, Kaminsky VA. Prog React Kinet 1994;19:139.
[176] Buback M, Busch M, Kowollik C. Macromol Theor Simul 2000;9:442.
[177] Fischer H, Baer R, Hany R, Verhoolen I, Walbiner M. J Chem Soc, Perkin Trans 2 1990:787.
[178] Buback M, Barner-Kowollik C, Egorov M, Kaminsky V. Macromol Theor Simul 2001;10:209.
[179] Khokhlov AR. Makromol Chem Rapid Commun 1981;2:633.
[180] Mahabadi HK. Macromolecules 1985;18:1319.
[181] Olaj OF, Schnöll-Bitai I, Kremminger P. Eur Polym J 1989;25:535.

[182] Davis TP, O'Driscoll KF, Piton MC, Winnik MA. J Polym Sci, Part C: Polym Lett 1989;27:181.
[183] Coote ML, Johnston LPM, Davis TP. Macromolecules 1997;30:8191.
[184] Davis TP, O'Driscoll KF, Piton MC, Winnik MA. Macromolecules 1990;23:2113.
[185] Beuermann S, Buback M, Busch M. Free-radical polymerization in reactive supercritical fluids. In: Jessop PG, Leitner W, editors. Chemical synthesis using supercritical fluids. Weinheim: Wiley–VCH, 1999. p. 326.